

MATHICSE Technical Report
Nr. 34 .2016 NEW
August 2016 (July 2017/November 2017)



Numerical homogenization and
model order reduction for
multiscale inverse problems

Assyr Abdulle, Andrea Di Blasio

NUMERICAL HOMOGENIZATION AND MODEL ORDER REDUCTION FOR MULTISCALE INVERSE PROBLEMS

ASSYR ABDULLE* AND ANDREA DI BLASIO†

Abstract. A new numerical method based on numerical homogenization and model order reduction is introduced for the solution of multiscale inverse problems. We consider a class of elliptic problems with highly oscillatory tensors that varies on a microscopic scale. We assume that the micro structure is known and seek to recover a macroscopic scalar parametrization of the microscale tensor (e.g. volume fraction). Departing from the full fine scale model that would require mesh resolution for the forward problem down to the finest scale, we solve the inverse problem for a coarse model obtained by numerical homogenization. The input data, i.e., measurement from the Dirichlet to Neumann map, are solely based on the original fine scale model. Furthermore, reduced basis techniques are used to avoid computing effective coefficients for the forward solver at each integration point of the macroscopic mesh. Uniqueness and stability of the effective inverse problem is established based on standard assumptions for the fine scale model and a link with this latter model is established by means of G-convergence. A priori error estimates are established for our method. Numerical experiments illustrate the efficiency of the proposed scheme and confirm our theoretical finding.

Key words. Inverse problems, Homogenization, Multiscale methods, Reduced basis.

AMS subject classifications. 65N21, 65N30, 35R30, 35B40

1. Introduction. Many applications in engineering and the sciences require solving inverse problems for partial differential equations (PDEs). We mention applications in heat conduction, geoscience and wave scattering, medical imaging, etc [14]. In this paper we are interested in PDEs that vary on very fine scale that come, e.g., from heterogeneity in the medium. Assuming that the nature of the micro structure is known, we search for an unknown macroscopic parametrization of this fine scale structure from the knowledge of measurements coming from the Dirichlet to Neumann map. A typical example is multi-phase medium whose constituents are known but whose volume fraction or its macroscopic orientation are unknown. Classical approaches for such problem would require the resolution of forward problems requiring mesh resolution of the fines scale. Repeated solutions of such high dimensional problem represent a formidable computational challenge and is often not tractable. Using coarse graining techniques and model order reduction can overcome this computational issue for classes of multiscale PDEs. Among such problems we consider the following multiscale elliptic problem. Let $\Omega \in \mathbb{R}^d$, $d \geq 2$, be an open, bounded, connected set with sufficiently smooth boundary $\partial\Omega$ and consider the problem of finding the weak solution $u^\varepsilon \in H^1(\Omega)$ to

$$(1.1) \quad \begin{aligned} -\nabla \cdot (A^\varepsilon \nabla u^\varepsilon) &= 0 && \text{in } \Omega, \\ u^\varepsilon &= g && \text{on } \partial\Omega, \end{aligned}$$

where $g \in H^{1/2}(\partial\Omega)$. The tensor $A^\varepsilon = A^\varepsilon(x)$, $x \in \Omega$ belongs to $\mathcal{M}(\alpha, \beta, \Omega)$, where

$$\mathcal{M}(\alpha, \beta, \Omega) := \{A \in L^\infty(\Omega, \text{Sym}_d) : \alpha|\xi|^2 \leq A(x)\xi \cdot \xi, |A(x)\xi| \leq \beta|\xi|, \forall \xi \in \mathbb{R}^d, \text{ and a.e. } x \in \Omega\},$$

*École Polytechnique Fédérale de Lausanne, Switzerland (assyр.abdulle@epfl.ch),

†École Polytechnique Fédérale de Lausanne, Switzerland(andrea.diblasio@epfl.ch)

where Sym_d denotes the class of $d \times d$ real valued symmetric matrices. The superscript in A^ε indicates that the tensor varies on a fine scale ε that is much smaller than the size of the computational domain Ω . In turn, the solution of (1.1) itself has variations on such micro scales.

Next, we introduce the Dirichlet to Neumann map associated to the boundary value problem (1.1) as the operator $\Lambda_{A^\varepsilon} : H^{1/2}(\partial\Omega) \rightarrow H^{-1/2}(\partial\Omega)$ given by

$$g \mapsto A^\varepsilon \nabla u^\varepsilon \cdot \nu|_{\partial\Omega},$$

where ν denotes the exterior unit normal to $\partial\Omega$. In this work we are concerned with the inverse conductivity problem of determining A^ε from the knowledge of the Dirichlet to Neumann map Λ_{A^ε} . The inverse conductivity problem, which is also known as electrical impedance tomography (EIT), was proposed firstly by Calderón [11], and it has gained great popularity in the last decades. Many authors have studied important questions that arise when facing the inverse conductivity problem, such as uniqueness of A^ε given Λ_{A^ε} , the recovery of A^ε from Λ_{A^ε} , and finally the stability or continuity of the inverse map $\Lambda_{A^\varepsilon} \mapsto A^\varepsilon$ [8, 27, 29, 33].

We mention that multiscale inverse problems for elliptic equations have already been treated in [30]. However there the authors are interested in recovering the effective tensor A^0 given some measurements of the full fine scale solution u^ε in the domain's interior. Moreover no use of numerical homogenization is employed. Here instead our measurements consists of multiscale fluxes at the boundary, and we use numerical homogenization to retrieve low dimensional parameters in order to recover the full multiscale tensor A^ε . Hence the setting is different from the one considered in our paper, as well as the theoretical and numerical results. We also mention the work [15], where a geometric framework for homogenization and inverse homogenization is introduced. The numerical method builds on harmonic coordinate transformations which require to solve multiple fine scale problems over the whole domain. Again this setting differs from the one we propose in our contribution.

In this paper we are interested in a class of parametrized anisotropic locally periodic multiscale tensor $A^\varepsilon(x) = A(\sigma^*(x), x/\varepsilon) = A(\sigma^*(x), y)$ Y -periodic in the y variable (here without loss of generality we assume that Y is a cube $Y = (0, 1)^d$). The map $(t, x) \mapsto A(t, x/\varepsilon)$ is assumed to be known and σ^* has to be determined. When the tensor does not exhibit a multiscale variation, i.e., for $(t, x) \mapsto A(t, x)$, uniqueness and stability at the boundary were proved by G. Alessandrini and R. Gaburro [7], under some regularity assumptions on the map $(t, x) \mapsto A(t, x)$. While this results is still valid for highly oscillating tensors, the stability estimates will depend on a constant that scales as $\mathcal{O}(\varepsilon^{-1})$. In turn, classical numerical techniques such as finite element methods (FEMs) to compute numerically the inverse problem will need scale resolution (i.e. mesh size resolving the smallest scale ε) which represents often a prohibitive cost. Therefore we combine the inverse problem with a coarse grained strategy, which simplifies remarkably the computational effort, but on the other hand introduces additional discrepancies between “reality” (model (1.1), from where the data are obtained) and the model used for inversion.

Homogenization theory [9, 25] ensures that the solution to problem (1.1) converges (in a weak sense) to a homogenized solution u^0 , solving the elliptic problem

$$(1.2) \quad \begin{aligned} -\nabla \cdot (A^0 \nabla u^0) &= 0 && \text{in } \Omega, \\ u^0 &= g && \text{on } \partial\Omega. \end{aligned}$$

In this work we want to analyse the possibility of retrieving A^ε , in the case where

the observed data are obtained from the full multiscale model (1.1), but using as forward model the Dirichlet to Neumann map defined by the homogenized model (1.2). Numerically, the explicit form of A^0 is usually not known and can only be recovered at some quadrature points of the macroscopic computational mesh. We therefore rely on the finite element heterogeneous multiscale method (FE-HMM) [1, 3, 5] that recovers such tensors with input data only given by the fine scale model (1.1), by solving appropriate micro problems. Furthermore, as such coarse grain forward solution relies on increasingly accurate micro solutions, we further employ reduced basis techniques to precompute a reduced number of conductivity tensors that are then appropriately interpolated when solving the forward problem following the methodology developed in [4].

This type of multiscale inverse problem has first been introduced in [19], where by means of numerical investigation, it is shown that the numerical homogenization can be used for the considered class of multiscale inverse problems. In our paper, we generalize the applicability of the numerical homogenization, we provide a theoretical investigation both on the model problem and on the computational approach for such coarse graining strategy and we further introduce model reduction strategy for the numerical method. We briefly discuss the main contribution of our paper. First, while in [19] it assumed that the scalar parameter σ^* is accurately parametrized by piecewise smooth coefficients, we consider instead general scalar parameter where no specific form of $t \rightarrow A(t, x/\varepsilon)$ is taken into account. Second, assuming that the fine scale inverse problem is well posed, we show that the effective inverse problem, with observed data consisting of the homogenized Dirichlet to Neumann map, is also well posed and we establish stability results independent of the small scale ε . As the full Dirichlet to Neumann map is usually not available, we discuss a numerical strategy based on finite measurements of this map. For our more general class of multiscale tensors, regularization is needed and we analyse this strategy in the context of multiscale inverse problems. Then in this framework, by means of G-convergence, we characterize the convergence of the solution of the effective inverse problem with multiscale observations as $\varepsilon \rightarrow 0$. Finally we provide a new numerical strategy based on the HMM framework and reduced basis techniques for solving the inverse problem. A priori error estimates for the computation of effective boundary fluxes is analysed for this method and convergence of the discrete optimization problem is established. The outline of the work is as follows. In Section 2 we recall briefly results of uniqueness and stability for the class of inverse problems that we consider, and we give motivation for the need of a coarse graining strategy to solve the inverse problem. In Section 3 we establish a convergence result for the solution to the inverse problem in the context of Tikhonov regularization. In Section 4 we describe how the multiscale inverse problem is solved numerically. In particular, we introduce numerical homogenization and we give a priori error estimates for the approximated flux at the boundary. An analysis on the discrete solution of the multiscale inverse problem is also given. Finally in Section 5 we present some numerical results to test our theoretical findings and illustrate our numerical method.

2. Calderón’s problem, multiscale data and homogenization. Let Ω be an open bounded set in \mathbb{R}^d and let $A^\varepsilon(x)$ be of the form $A(\sigma^*(x), x/\varepsilon)$, for a certain scalar function $\sigma^* : \Omega \rightarrow \mathbb{R}$. The problem we are interested in is to recover the function σ^* from measurements of the Dirichlet to Neumann map, in order to retrieve the full conductivity tensor A^ε . The inverse conductivity problem was firstly introduced by Calderón [11], while inverse conductivity problems for special anisotropic tensors of

the form $A(x) = A(\sigma^*(x), x)$ are analysed in details in [7]. In particular in [7] results on uniqueness and stability at the boundary for the inverse problem are proved in the case where some prior knowledge on the map $(t, x) \mapsto A(t, x)$ is assumed. It is required that the tensor $A(t, x)$, $t \in [\sigma^-, \sigma^+]$, $0 < \sigma^- < \sigma^+$, $x \in \Omega$, belongs to some special class of matrix functions that we recall below. In what follows we will use the following norms

$$\|A\|_{L^p(\Omega)} = \left(\int_{\Omega} \sum_{i=1}^d \sum_{j=1}^d |a_{ij}(x)|^p dx \right)^{1/p}, \quad 1 \leq p < \infty,$$

$$\|A\|_{L^\infty(\Omega)} = \max_{1 \leq i, j \leq d} \operatorname{ess\,sup}_{x \in \Omega} |a_{ij}(x)|, \quad p = \infty.$$

for a matrix $A(x) = \{a_{ij}(x)\}_{1 \leq i, j \leq d}$, $x \in \Omega$.

DEFINITION 2.1. [Definition 2.2 in [7]]. Given $p > d$, $\alpha, \beta, E_1 > 0$, and denoting by Sym_d the class of $d \times d$ real valued symmetric matrices, we say that $A : [\sigma^-, \sigma^+] \times \Omega \rightarrow Sym_d$ belongs to \mathcal{H} if the following conditions hold for all $t \in [\sigma^-, \sigma^+]$, $0 < \sigma^- < \sigma^+$:

1. $A \in W^{1,p}([\sigma^-, \sigma^+] \times \Omega, Sym_d)$.
2. $\partial_t A \in W^{1,p}([\sigma^-, \sigma^+] \times \Omega, Sym_d)$.
3. $\operatorname{ess\,sup}_{t \in [\sigma^-, \sigma^+]} (\|A(t, \cdot)\|_{L^p(\Omega)} + \|\nabla_x A(t, \cdot)\|_{L^p(\Omega)} + \|\partial_t A(t, \cdot)\|_{L^p(\Omega)} + \|\partial_t \nabla_x A(t, \cdot)\|_{L^p(\Omega)}) \leq E_1$.
4. Condition of uniform ellipticity:

$$\alpha|\xi|^2 \leq A(t, x)\xi \cdot \xi, |A(t, x)\xi| \leq \beta|\xi|, \quad \text{for a.e. } x \in \Omega$$

$$\text{and } \forall t \in [\sigma^-, \sigma^+], \xi \in \mathbb{R}^d.$$

5. Condition of monotonicity with respect to the variable t :

$$\partial_t A(t, x)\xi \cdot \xi \geq E_1^{-1}|\xi|^2, \quad \text{for a.e. } x \in \Omega$$

$$\text{and } \forall t \in [\sigma^-, \sigma^+], \xi \in \mathbb{R}^d.$$

In [7] the following stability result at the boundary for the unknown function σ^* has been shown, in the case where $A(x) = A(\sigma^*(x), x)$, $\sigma^* \in W^{1,p}(\Omega)$, $A(\cdot, \cdot) \in \mathcal{H}$.

THEOREM 2.2. [Theorem 2.1 in [7]]. Given $p > d$, let Ω be a bounded domain with Lipschitz boundary. Given $E > 0$, let σ_1, σ_2 satisfy

$$(2.1) \quad \sigma^- \leq \sigma_1(x), \sigma_2(x) \leq \sigma^+ \quad \text{for every } x \in \Omega,$$

and

$$(2.2) \quad \|\sigma_1\|_{W^{1,p}(\Omega)}, \|\sigma_2\|_{W^{1,p}(\Omega)} \leq E.$$

Let $A(\cdot, \cdot) \in \mathcal{H}$. Then we have

$$\|A(\sigma_1(x), x) - A(\sigma_2(x), x)\|_{L^\infty(\partial\Omega)} \leq C \|\Lambda_{A(\sigma_1, x)} - \Lambda_{A(\sigma_2, x)}\|_{\mathcal{L}(H^{1/2}(\partial\Omega), H^{-1/2}(\partial\Omega))},$$

where C depends on σ^-, σ^+, E, p , and Ω .

A uniqueness result is also provided in [7].

THEOREM 2.3. [Theorem 2.4 in [7]]. Given $E > 0$, let be σ_1 and σ_2 two scalar functions satisfying (2.1) and (2.2) with $p = \infty$, and $A(\cdot, \cdot) \in \mathcal{H}$. Moreover assume

$A \in W^{1,\infty}([\sigma^-, \sigma^+] \times \Omega, \text{Sym}_d)$. In addition, suppose that Ω can be partitioned into a finite number of Lipschitz domains $\{\Omega_j\}_{j=1}^N$ such that $\sigma_1 - \sigma_2$ is analytic on each $\overline{\Omega}_j$. If

$$\Lambda_{A(\sigma_1, x)} = \Lambda_{A(\sigma_2, x)}$$

then we have

$$A(\sigma_1(x), x) = A(\sigma_2(x), x) \quad \text{in } \Omega.$$

The same results hold for matrix functions of the type $A^\varepsilon(x) = A(\sigma^*(x), x/\varepsilon)$, for fixed ε . However in this case the constant E_1 in Definition 2.1 scales as $1/\varepsilon$, and therefore as $\varepsilon \rightarrow 0$, such results may become useless. Moreover, in numerical experiments, when ε is very small, trying to solve the problem numerically by using as model for inversion an approximation of (1.1) is prohibitive in terms of computational cost, and therefore a different strategy has to be preferred. Then the motivation for a coarse graining approach which we obtain by using the framework of homogenization.

DEFINITION 2.4. Let $\{A^\varepsilon\}_{\varepsilon>0}$ be a sequence of matrices in $\mathcal{M}(\alpha, \beta, \Omega)$. We say that it G -converges to the matrix $A^0 \in \mathcal{M}(\alpha, \beta, \Omega)$ iff for every function $f \in H^{-1}(\Omega)$, $g \in H^{1/2}(\partial\Omega)$, the solution u^ε of

$$(2.3) \quad \begin{aligned} -\nabla \cdot (A^\varepsilon \nabla u^\varepsilon) &= f && \text{in } \Omega, \\ u^\varepsilon &= g && \text{on } \partial\Omega, \end{aligned}$$

is such that

$$u^\varepsilon \rightharpoonup u^0 \quad \text{weakly in } H^1(\Omega),$$

where u^0 is the unique solution of

$$(2.4) \quad \begin{aligned} -\nabla \cdot (A^0 \nabla u^0) &= f && \text{in } \Omega, \\ u^0 &= g && \text{on } \partial\Omega. \end{aligned}$$

Moreover in the symmetric case we have that

$$A^\varepsilon \nabla u^\varepsilon \rightharpoonup A^0 \nabla u^0 \quad \text{weakly in } (L^2(\Omega))^d.$$

THEOREM 2.5. One has the following compactness result. Let $\{A^\varepsilon\}_{\varepsilon>0}$ be a sequence of matrices in $\mathcal{M}(\alpha, \beta, \Omega)$. Then there exists a subsequence $\{A^{\varepsilon'}\}_{\varepsilon'>0}$ and a matrix $A^0 \in \mathcal{M}(\alpha, \beta, \Omega)$ such that $\{A^{\varepsilon'}\}_{\varepsilon'>0}$ G -converges to A^0 .

In particular let us consider for now the case where A^ε is the Y -periodic matrix defined by

$$A^\varepsilon(x) = A(x, x/\varepsilon) = A(x, y), \quad A(x, \cdot) \in \mathcal{M}(\alpha, \beta, Y), \forall x \in \Omega,$$

$$A^\varepsilon(x) = \{a_{ij}^\varepsilon(x)\}_{1 \leq i, j \leq d} \quad \text{a.e. on } \mathbb{R}^d,$$

where

$$a_{ij}^\varepsilon(x) = a_{ij}(x, x/\varepsilon) = a_{ij}(x, y), \quad a_{ij}(x, \cdot) \text{ is } Y\text{-periodic}, \forall x \in \Omega, \forall i, j = 1, \dots, d,$$

where Y denotes the reference unit cell $(0, 1)^d$.

In this particular case we have that the whole sequence $\{A^\varepsilon\}_{\varepsilon>0}$ G-converges to the tensor $A^0 \in \mathcal{M}(\alpha, \beta, \Omega)$, $A^0(x) = \{a_{ij}^0(x)\}_{1 \leq i, j \leq d}$, which is elliptic and it is given by

$$a_{ij}^0(x) = \frac{1}{|Y|} \int_Y a_{ij}(x, y) \, dy - \frac{1}{|Y|} \sum_{k=1}^d \int_Y a_{ik}(x, y) \frac{\partial \chi_j}{\partial y_k} \, dy \quad \forall i, j = 1, \dots, d.$$

The micro functions χ_j , $j = 1, \dots, d$, are defined to be the unique solutions of the cell problems: find $\chi_j \in W_{per}^1(Y)$ such that

$$(2.5) \quad \int_Y A(x, y) \nabla_y \chi_j \cdot \nabla_y v \, dy = \int_Y A(x, y) \mathbf{e}_j \cdot \nabla_y v \, dy, \quad \forall v \in W_{per}^1(Y),$$

where $\{\mathbf{e}_j\}_{j=1}^d$ is the canonical basis of \mathbb{R}^d and

$$W_{per}^1(Y) = \left\{ v \in H_{per}^1(Y) : \int_Y v \, dy = 0 \right\},$$

where $H_{per}^1(Y)$ is defined as the closure of $C_{per}^\infty(Y)$ for the H^1 -norm (where $C_{per}^\infty(Y)$ denotes the subset of $C^\infty(\mathbb{R}^d)$ of periodic functions in Y). In definition 2.1 we have listed the regularity properties that the map $(t, x) \mapsto A(t, x/\varepsilon)$ has to satisfy to ensure stability and uniqueness of the inverse problem. However we already mentioned that for the class of problems we are interested in, results obtained in [7] are dependent of ε , and a new strategy based on homogenization is preferred. As first step we want to analyse under which conditions on A^ε , the map $t \mapsto A^0(t)$ satisfies the regularity properties to ensure stability and uniqueness for the homogenized inverse problem. First, let us introduce as a corollary of Theorem 2.2 and 2.3 the conditions that A^0 has to satisfy to ensure stability and uniqueness.

COROLLARY 2.6. *Given $\alpha, \beta, E_2 > 0$ and $p > d$, let us consider a $d \times d$ symmetric matrix valued function $t \mapsto A(t)$, $t \in [\sigma^-, \sigma^+]$, $0 < \sigma^- < \sigma^+$, satisfying the conditions*

$$(2.6) \quad |\partial_t A(t)| + |\partial_t^2 A(t)| \leq E_2, \quad \forall t \in [\sigma^-, \sigma^+].$$

$$(2.7) \quad \alpha |\xi|^2 \leq A(t) \xi \cdot \xi, |A(x) \xi| \leq \beta |\xi|, \quad \forall t \in [\sigma^-, \sigma^+], \xi \in \mathbb{R}^d.$$

$$(2.8) \quad \partial_t A(t) \xi \cdot \xi \geq E_2^{-1} |\xi|^2, \quad \forall t \in [\sigma^-, \sigma^+], \xi \in \mathbb{R}^d.$$

Let σ_1 and σ_2 two scalar functions satisfying (2.1)-(2.2). Then we have the following results.

1. The following estimate holds:

$$\|A(\sigma_1) - A(\sigma_2)\|_{L^\infty(\partial\Omega)} \leq C \|\Lambda_{A(\sigma_1)} - \Lambda_{A(\sigma_2)}\|_{\mathcal{L}(H^{1/2}(\partial\Omega), H^{-1/2}(\partial\Omega))},$$

where C depends on σ^-, σ^+, E, p , and Ω .

2. Let σ_1 and σ_2 satisfy (2.1) and (2.2) with $p = \infty$. In addition suppose that Ω can be partitioned into a finite number of Lipschitz domains $\{\Omega_j\}_{j=1}^N$ such that $\sigma_1 - \sigma_2$ is analytic on each $\overline{\Omega}_j$. If

$$\Lambda_{A(\sigma_1)} = \Lambda_{A(\sigma_2)}$$

then we have

$$A(\sigma_1) = A(\sigma_2) \quad \text{in } \Omega.$$

We also mention the following lemma which establishes a regularity result for the solutions of the cell problems (2.5) with respect to the variable t [6].

LEMMA 2.7. *Assume that $A(t, x/\varepsilon)$ is uniformly elliptic and the map $t \mapsto A(t, x/\varepsilon)$ is of class $C^1([\sigma^-, \sigma^+], \text{Sym}_d)$. Consider the micro functions $\chi_j(t, y)$, $j = 1, \dots, d$, unique solutions of: find $\chi_j \in W_{per}^1(Y)$ such that*

$$(2.9) \quad \int_Y A(t, y) \nabla_y \chi_j \cdot \nabla_y v \, dy = \int_Y A(t, y) \mathbf{e}_j \cdot \nabla_y v \, dy \quad \forall v \in W_{per}^1(Y).$$

Then the map $t \mapsto \chi_j(t, y) \in W_{per}^1(Y)$ is of class $C^1([\sigma^-, \sigma^+])$ and satisfies

$$(2.10) \quad \partial_t \chi_j(t, y) = \phi_j(t, y), \quad \partial_t \nabla_y \chi_j(t, y) = \nabla_y \phi_j(t, y),$$

where $\phi_j(t, y) \in W_{per}^1(Y)$ and satisfies

$$\int_Y A(t, y) \nabla_y \phi_j(t, y) \cdot \nabla_y v \, dy = \int_Y \partial_t A(t, y) (\mathbf{e}_j - \nabla_y \chi_j(t, y)) \cdot \nabla_y v \, dy \quad \forall v \in W_{per}^1(Y).$$

Then we can establish the following theorem whose proof is given in the appendix.

THEOREM 2.8. *Let $x/\varepsilon = y \in Y$. Given $\alpha, \beta, E_1 > 0$, $p > d$, consider the class of $d \times d$ symmetric matrix functions $(t, y) \mapsto A(t, y)$, where a_{ij} is Y -periodic, $\forall i, j = 1, \dots, d$, $t \in [\sigma^-, \sigma^+]$, $0 < \sigma^- < \sigma^+$. Assume*

$$(2.11) \quad A \in W^{1, \infty}([\sigma^-, \sigma^+] \times Y, \text{Sym}_d), \quad \|A\|_{W^{1, \infty}([\sigma^-, \sigma^+]; W^{1, \infty}(Y))} \leq E_1.$$

$$(2.12) \quad \partial_t A \in W^{1, \infty}([\sigma^-, \sigma^+] \times Y, \text{Sym}_d), \quad \|\partial_t A\|_{W^{1, \infty}([\sigma^-, \sigma^+]; W^{1, \infty}(Y))} \leq E_1.$$

$$(2.13) \quad \alpha |\xi|^2 \leq A(t, y) \xi \cdot \xi, \quad |A(x) \xi| \leq \beta |\xi|, \quad \text{for a.e. } y \in Y \text{ and } \forall t \in [\sigma^-, \sigma^+], \xi \in \mathbb{R}^d.$$

$$(2.14) \quad \partial_t A(t, y) \xi \cdot \xi \geq E_1^{-1} |\xi|^2, \quad \text{for a.e. } y \in Y \text{ and } \forall t \in [\sigma^-, \sigma^+], \xi \in \mathbb{R}^d.$$

Then the homogenized tensor A^0 satisfies (2.6)-(2.8).

Hence, under appropriate regularity assumptions on A^ε , we established stability and uniqueness for the inverse conductivity problem in the case the measurements at the boundary consist of the homogenized Dirichlet to Neumann map. However, as already mentioned in the introduction, this is not the case we are interested in, since we aim at solving the inverse problem when the data consists of the multiscale Dirichlet to Neumann map $\Lambda_{A(\sigma^*, x/\varepsilon)}$. Moreover in real experiments we do not have full knowledge of the map $\Lambda_{A(\sigma^*, x/\varepsilon)}$. Indeed we would have to know the results of all possible boundary measurements for any Dirichlet boundary conditions g , which is impossible. In practice, we consider a set of L experiments, described by a finite set of Dirichlet conditions $\{g_l\}_{l=1}^L \in H^{1/2}(\partial\Omega)$, and for each of them we measure the corresponding boundary flux. Let us define

$$U = \{\sigma \in W^{1, \infty}(\Omega) : \sigma^- \leq \sigma(x) \leq \sigma^+, 0 < \sigma^- < \sigma^+\},$$

$$U_{ad} = \{\sigma \in U : \|\sigma(x)\|_{W^{1, \infty}(\Omega)} \leq E, E > 0\}.$$

Then we would like to solve the following minimization problem

$$(2.15) \quad \min_{\sigma \in U_{ad}} \sum_{l=1}^L \|\Lambda_{A(\sigma^*, x/\varepsilon)} g_l - \Lambda_{A^0(\sigma)} g_l\|_{H^{-1/2}(\partial\Omega)}^2,$$

subject to

$$\begin{aligned} -\nabla \cdot (A^0(\sigma(x)) \nabla u^0) &= 0 && \text{in } \Omega, \\ u^0 &= g_l && \text{on } \partial\Omega, \end{aligned}$$

where $A^0(\sigma(x))$ is the homogenized tensor corresponding to $A(\sigma(x), x/\varepsilon)$. It is important to remark that G-convergence of $A(\sigma^*(x), x/\varepsilon)$ to $A^0(\sigma^*(x))$ does not imply convergence of the corresponding fluxes at the boundary in the $H^{-1/2}(\partial\Omega)$ -norm, but only weak* convergence, as stated in the following lemma.

LEMMA 2.9. *Let us consider a sequence of tensors $\{A^\varepsilon\}_{\varepsilon>0}$ in $\mathcal{M}(\alpha, \beta, \Omega)$ which G-converges to $A^0 \in \mathcal{M}(\alpha, \beta, \Omega)$ as $\varepsilon \rightarrow 0$. Then $\{\Lambda_{A^\varepsilon} g\}_{\varepsilon>0}$ converges weakly* to $\Lambda_{A^0} g$ in $H^{-1/2}(\partial\Omega)$ for all $g \in H^{1/2}(\partial\Omega)$ as $\varepsilon \rightarrow 0$.*

Proof. From the definition of G-convergence we have that, for any $\psi \in H^1(\Omega)$,

$$\int_{\Omega} (A^\varepsilon \nabla u^\varepsilon - A^0 \nabla u^0) \cdot \nabla \psi \, dx \rightarrow 0 \quad \text{as } \varepsilon \rightarrow 0,$$

where $u^\varepsilon, u^0 \in H^1(\Omega)$ are the weak solutions of (1.1) and (1.2) respectively. Then, using integration by parts, we obtain that

$$(2.16) \quad \langle \Lambda_{A^\varepsilon} g - \Lambda_{A^0} g, \psi \rangle_{H^{-1/2}(\partial\Omega), H^{1/2}(\partial\Omega)} \rightarrow 0 \quad \text{as } \varepsilon \rightarrow 0,$$

for each $g, \psi \in H^{1/2}(\partial\Omega)$. Then

$$\Lambda_{A^\varepsilon} g \rightharpoonup \Lambda_{A^0} g \quad \text{weakly* in } H^{-1/2}(\partial\Omega).$$

□

3. Tikhonov regularization, multiscale and coarse-grained minimizers.

Due to the difficulties of working with fractional-order Sobolev spaces when performing numerical experiments, we will consider the $L^2(\partial\Omega)$ -norm to evaluate the distance between data and numerical results produced by the homogenized model, where it is assumed $g_l \in H^{3/2}(\partial\Omega)$, $\forall l = 1, \dots, L$. Let $\Phi^\varepsilon : U \rightarrow \mathbb{R}$ be defined as

$$\Phi^\varepsilon(\sigma) = \sum_{l=1}^L \|\Lambda_{A(\sigma^*, x/\varepsilon)} g_l - \Lambda_{A^0(\sigma)} g_l\|_{L^2(\partial\Omega)}^2,$$

and let us consider the minimization problem

$$(3.1) \quad \overline{\Phi^\varepsilon} = \inf_{\sigma \in U_{ad}} \Phi^\varepsilon(\sigma).$$

Since U_{ad} is a closed convex and bounded set in $W^{1,\infty}(\Omega)$ it is possible to prove that any minimizing sequence $\{\sigma_n^\varepsilon\}_{n \geq 0}$ for (3.1) contains a subsequence which weakly converges to $\overline{\sigma^\varepsilon}$, for which we have $\overline{\Phi^\varepsilon} = \Phi^\varepsilon(\overline{\sigma^\varepsilon})$. The proof is quite standard. Let us recall that $H^1(\Omega)$ embeds compactly into $L^r(\Omega)$, $r < \infty$ in two dimensions, $r < 6$ in three dimensions. Then the key point consists in proving that $\Phi^\varepsilon : L^r(\Omega) \cap U \rightarrow \mathbb{R}^+$

is continuous. Such result is stated in the lemma below, whose proof is reported in the appendix.

LEMMA 3.1. *Let $A^0(\cdot)$ satisfy (2.6)-(2.7). Let the sequence $\{\sigma_n\}_{n>0} \subset U$ converge to some $\sigma \in U$ in $L^r(\Omega)$, $r \geq 1$. Then the sequence $\{\Lambda_{A^0(\sigma_n)}g\}_{n>0}$ converges to $\Lambda_{A^0(\sigma)}g$ in $H^{-1/2}(\partial\Omega)$. If $u^0 \in H^2(\Omega)$, then the sequence $\{\Lambda_{A^0(\sigma_n)}g\}_{n>0}$ converges to $\Lambda_{A^0(\sigma)}g$ in $L^2(\partial\Omega)$.*

However in numerical experiments we may prefer to adopt indirect methods to ensure stability of the inverse problem instead of directly impose a constraint during the minimization procedure. Among the possible methods to regularize inverse problems we choose Tikhonov regularization (see for example [16,18]). Tikhonov regularization ensures well posedness by adding to the cost functional a convex variational penalty, so that the new minimization problem reads.

$$(3.2) \quad \overline{\Psi^\varepsilon} = \inf_{\sigma \in U} \Psi^\varepsilon(\sigma)$$

where

$$(3.3) \quad \Psi^\varepsilon(\sigma) = \Phi^\varepsilon(\sigma) + \gamma R(\sigma),$$

where γ is the regularization parameter, and R is the penalty term. Such term induces a priori knowledge on expected conductivity. In what follows we consider $R(\sigma) = \|\sigma - \sigma_0\|_{H^1(\Omega)}^2$, where σ_0 is a prior guess of σ^* . The regularization parameter controls the trade-off between the two terms and has to be properly chosen. The choice of γ represents a problem of considerable interest and will affect how much oscillation is allowed in any minimizing sequence. As the regularization parameter γ varies, we obtain different regularized solutions having properties that vary with γ . However how to choose γ is not the main subject of study of this particular work. For sake of completeness we mention that several methods have been proposed in literature, as the Morozov's discrepancy principle [26,32] or the L-curve method [23,24]. Let us introduce the functional $\Psi^0 : U \rightarrow \mathbb{R}$, such that

$$(3.4) \quad \overline{\Psi^0} = \inf_{\sigma \in U} \Psi^0(\sigma)$$

where

$$\Psi^0(\sigma) = \Phi^0(\sigma) + \gamma \|\sigma - \sigma_0\|_{H^1(\Omega)}^2,$$

and

$$\Phi^0(\sigma) = \sum_{l=1}^L \|\Lambda_{A^0(\sigma^*)}g_l - \Lambda_{A^0(\sigma)}g_l\|_{L^2(\partial\Omega)}^2.$$

Remark. From the non-negativity of $\Psi^\varepsilon(\sigma)$ and $\Psi^0(\sigma)$, it follows that $\Psi^\varepsilon(U)$ and $\Psi^0(U)$ are subsets of \mathbb{R}^+ , and therefore there exist minimizing sequences $\{\sigma_n^\varepsilon\}_{n>0}$ and $\{\sigma_n^0\}_{n>0}$ such that

$$\begin{aligned} \overline{\Psi^\varepsilon} &= \liminf_{n \rightarrow \infty} \Psi^\varepsilon(\sigma_n^\varepsilon) = \inf_{\sigma \in U} \Psi^\varepsilon(\sigma), \\ \overline{\Psi^0} &= \liminf_{n \rightarrow \infty} \Psi^0(\sigma_n^0) = \inf_{\sigma \in U} \Psi^0(\sigma). \end{aligned}$$

The following lemma is an adaptation of a classical result in non-linear Tikhonov regularization theory (see e.g. [17]).

LEMMA 3.2. *Let $u^0 \in H^2(\Omega)$, and consider a minimizing sequence $\{\sigma_n^0\}_{n>0}$ for (3.4). Then it contains a weakly convergent subsequence in $H^1(\Omega)$ with limit $\bar{\sigma}^0 \in U$ which attains the infimum: $\bar{\Psi}^0 = \Psi^0(\bar{\sigma}^0)$.*

Proof. The set U is a non-empty closed convex subset of $H^1(\Omega)$, hence sequentially weakly closed. From the minimizing property of $\{\sigma_n^0\}_{n>0}$ and the non-negativity of $\Phi^0(\sigma)$ it follows that $\{\sigma_n^0\}_{n>0}$ is bounded in $H^1(\Omega)$. Indeed if this is not the case, there exists a subsequence $\{\sigma_{n'}^0\}_{n'>0}$ such that $\|\sigma_{n'}^0\|_{H^1(\Omega)} \rightarrow \infty$ as $n' \rightarrow \infty$, hence

$$\Psi^0(\sigma_{n'}^0) \geq \gamma \|\sigma_{n'}^0 - \sigma_0\|_{H^1(\Omega)}^2 \rightarrow \infty,$$

and therefore $\bar{\Psi}^0 = \infty$. Then $\{\sigma_n^0\}_{n>0}$ admits a subsequence $\{\sigma_{n'}^0\}_{n'>0}$ such that $\sigma_{n'}^0 \rightharpoonup \bar{\sigma}^0$ weakly in $H^1(\Omega)$. Since $\Phi^0 : L^r(\Omega) \cap U \rightarrow \mathbb{R}^+$ is continuous (Lemma 3.1) and the $H^1(\Omega)$ -norm is weakly lower semi-continuous we have that

$$\Psi^0(\bar{\sigma}^0) \leq \liminf_{n' \rightarrow \infty} \Psi^0(\sigma_{n'}^0) = \bar{\Psi}^0.$$

Since $\Psi^0(\bar{\sigma}^0) \geq \bar{\Psi}^0$, the result follows. \square

Using the same arguments the following lemma can also be proved.

LEMMA 3.3. *Let $u^0 \in H^2(\Omega)$, and consider a minimizing sequence $\{\sigma_n^\varepsilon\}_{n>0}$ for (3.2). Then it contains a weakly convergent subsequence in $H^1(\Omega)$ with limit $\bar{\sigma}^\varepsilon \in U$ which attains the infimum: $\bar{\Psi}^\varepsilon = \Psi^\varepsilon(\bar{\sigma}^\varepsilon)$.*

We now state the main result that quantifies (in a weak sense) the link between the minimization problem (3.2) involving the fine scale Dirichlet to Neumann map $\Lambda_{A(\sigma^*, x/\varepsilon)}$ and the homogenized map $\Lambda_{A^0(\sigma^*)}$, and the problem (3.4) involving only homogenized maps.

THEOREM 3.4. *Consider the sequence of minimization problems of type (3.2) for $\varepsilon \rightarrow 0$. The sequence of minimizers $\{\bar{\sigma}^\varepsilon\}_{\varepsilon>0}$, such that $\bar{\Psi}^\varepsilon = \Psi^\varepsilon(\bar{\sigma}^\varepsilon)$ for all $\varepsilon > 0$, contains a weakly convergent subsequence in $H^1(\Omega)$ with limit $\bar{\sigma} \in U$ which attains the infimum: $\bar{\Psi}^0 = \Psi^0(\bar{\sigma})$.*

Proof. The minimizing property of $\{\bar{\sigma}^\varepsilon\}_{\varepsilon>0}$ and the non-negativity of $\Phi^\varepsilon(\sigma)$ imply that the sequence $\{\bar{\sigma}^\varepsilon\}_{\varepsilon>0}$ is bounded in $H^1(\Omega)$. Indeed we have that for each $\varepsilon > 0$, $\Psi^\varepsilon(\bar{\sigma}^\varepsilon)$ is bounded by $\Psi^\varepsilon(\sigma^*)$, which is in turn bounded with respect to ε . From calculations similar as in the proof of Lemma 3.1 we obtain

$$\begin{aligned} \Psi^\varepsilon(\sigma^*) &= \sum_{l=1}^L \|\Lambda_{A(\sigma^*, x/\varepsilon)} g_l - \Lambda_{A^0(\sigma^*)} g_l\|_{L^2(\partial\Omega)}^2 + \gamma \|\sigma^* - \sigma_0\|_{H^1(\Omega)}^2 \\ &\leq \sum_{l=1}^L 2\beta^2 \|g_l\|_{H^{3/2}(\partial\Omega)}^2 + \gamma \|\sigma^* - \sigma_0\|_{H^1(\Omega)}^2. \end{aligned}$$

Then $\{\bar{\sigma}^\varepsilon\}_{\varepsilon>0}$ admits a subsequence $\{\bar{\sigma}^{\varepsilon'}\}_{\varepsilon'>0}$ which converges weakly in $H^1(\Omega)$ to some $\bar{\sigma} \in U$. We know that

$$(3.5) \quad \Psi^{\varepsilon'}(\bar{\sigma}^{\varepsilon'}) \leq \Psi^{\varepsilon'}(\bar{\sigma}^0) \quad \forall \varepsilon' > 0.$$

Moreover for each $\sigma \in U$ and $\varepsilon > 0$ the following identity holds

$$(3.6) \quad \begin{aligned} \Psi^\varepsilon(\sigma) &= \Phi^\varepsilon(\sigma^*) + \Phi^0(\sigma) + \gamma \|\sigma - \sigma_0\|_{H^1(\Omega)}^2 \\ &+ 2 \sum_{l=1}^L \langle \Lambda_{A(\sigma^*, x/\varepsilon)} g_l - \Lambda_{A^0(\sigma^*)} g_l, \Lambda_{A^0(\sigma^*)} g_l - \Lambda_{A^0(\sigma)} g_l \rangle_{L^2(\partial\Omega), L^2(\partial\Omega)}. \end{aligned}$$

Inserting (3.6) into (3.5) we obtain

$$\Psi^0(\bar{\sigma}^{\varepsilon'}) \leq \Psi^0(\bar{\sigma}^0) + 2 \sum_{l=1}^L \langle \Lambda_{A(\sigma^*, x/\varepsilon')} g_l - \Lambda_{A^0(\sigma^*)} g_l, \Lambda_{A^0(\bar{\sigma}^{\varepsilon'})} g_l - \Lambda_{A^0(\bar{\sigma}^0)} g_l \rangle_{L^2(\partial\Omega), L^2(\partial\Omega)}.$$

From Lemma 3.1 and the weak lower semi-continuity of the $H^1(\Omega)$ -norm we have that

$$\begin{aligned} \Psi^0(\bar{\sigma}) &\leq \liminf_{\varepsilon' \rightarrow 0} \Psi^0(\bar{\sigma}^{\varepsilon'}) \\ &\leq \liminf_{\varepsilon' \rightarrow 0} \left(\Psi^0(\bar{\sigma}^0) + 2 \sum_{l=1}^L \langle \Lambda_{A(\sigma^*, x/\varepsilon')} g_l - \Lambda_{A^0(\sigma^*)} g_l, \Lambda_{A^0(\bar{\sigma}^{\varepsilon'})} g_l - \Lambda_{A^0(\bar{\sigma}^0)} g_l \rangle_{L^2(\partial\Omega), L^2(\partial\Omega)} \right) \\ &\leq \Psi^0(\bar{\sigma}^0) \\ &\quad + \limsup_{\varepsilon' \rightarrow 0} 2 \sum_{l=1}^L \langle \Lambda_{A(\sigma^*, x/\varepsilon')} g_l - \Lambda_{A^0(\sigma^*)} g_l, \Lambda_{A^0(\bar{\sigma}^{\varepsilon'})} g_l \rangle_{L^2(\partial\Omega), L^2(\partial\Omega)} \\ &\quad + \limsup_{\varepsilon' \rightarrow 0} 2 \sum_{l=1}^L \langle \Lambda_{A(\sigma^*, x/\varepsilon')} g_l - \Lambda_{A^0(\sigma^*)} g_l, -\Lambda_{A^0(\bar{\sigma}^0)} g_l \rangle_{L^2(\partial\Omega), L^2(\partial\Omega)}. \end{aligned}$$

Using G-convergence of $A(\sigma^*(x), x/\varepsilon)$ to $A^0(\sigma^*(x))$ one obtains that

$$\begin{aligned} \Psi^0(\bar{\sigma}) &\leq \Psi^0(\bar{\sigma}^0) \\ &\quad + \limsup_{\varepsilon' \rightarrow 0} 2 \sum_{l=1}^L \langle \Lambda_{A(\sigma^*, x/\varepsilon')} g_l - \Lambda_{A^0(\sigma^*)} g_l, \Lambda_{A^0(\bar{\sigma}^{\varepsilon'})} g_l \rangle_{L^2(\partial\Omega), L^2(\partial\Omega)} \\ &\leq \Psi^0(\bar{\sigma}^0) \\ &\quad + \limsup_{\varepsilon' \rightarrow 0} 2 \sum_{l=1}^L \langle \Lambda_{A(\sigma^*, x/\varepsilon')} g_l - \Lambda_{A^0(\sigma^*)} g_l, \Lambda_{A^0(\bar{\sigma})} g_l \rangle_{L^2(\partial\Omega), L^2(\partial\Omega)} \\ &\quad + \limsup_{\varepsilon' \rightarrow 0} 2 \sum_{l=1}^L \langle \Lambda_{A(\sigma^*, x/\varepsilon')} g_l - \Lambda_{A^0(\sigma^*)} g_l, \Lambda_{A^0(\bar{\sigma}^{\varepsilon'})} g_l - \Lambda_{A^0(\bar{\sigma})} g_l \rangle_{L^2(\partial\Omega), L^2(\partial\Omega)} \\ &\leq \Psi^0(\bar{\sigma}^0) \\ &\quad + \limsup_{\varepsilon' \rightarrow 0} 4 \sum_{l=1}^L \beta \|g_l\|_{H^{3/2}(\partial\Omega)} \|\Lambda_{A^0(\bar{\sigma}^{\varepsilon'})} g_l - \Lambda_{A^0(\bar{\sigma})} g_l\|_{L^2(\partial\Omega)} \\ &= \Psi^0(\bar{\sigma}^0) = \bar{\Psi}^0. \end{aligned}$$

Since $\Psi^0(\bar{\sigma}) \geq \bar{\Psi}^0$, the result follows. \square

As consequence we have that $\Psi^0(\bar{\sigma}^\varepsilon) \rightarrow \Psi^0(\bar{\sigma}^0)$ up to a subsequence when $\varepsilon \rightarrow 0$. Hence we have established a link between the solutions to the multiscale problem (3.2) and the solutions to the coarse grained minimization problem (3.4).

4. Numerical solution of the inverse problem. In this section we discuss the numerical solution of the inverse conductivity problem. At first we describe the forward solver employed to approximate the homogenized boundary flux. Given the problem

$$(4.1) \quad \begin{aligned} -\nabla \cdot (A^\varepsilon \nabla u^\varepsilon) &= f && \text{in } \Omega, \\ u^\varepsilon &= g && \text{on } \partial\Omega, \end{aligned}$$

we need an efficient method to evaluate the boundary flux $\Lambda_{A^0} g$ for the homogenized tensor A^0 . However given A^ε , analytic solutions for the corresponding A^0 are usually not available, hence we need numerical homogenization.

4.1. Numerical homogenization. For the numerical homogenization procedure, we choose the Finite Element Heterogeneous Multiscale Method (FE-HMM) which approximates the homogenized problem originating from (4.1) taking as input only the multiscale data. The FE-HMM it has been studied extensively in literature and for more details we refer to [1, 3, 5]. We state here the simplest version involving only piecewise linear macro and micro elements. The method is based on a macro finite element space

$$(4.2) \quad S_0^1(\Omega, \mathcal{T}_H) = \{v^H \in H_0^1(\Omega) : v^H|_K \in \mathcal{P}^1(K), \forall K \in \mathcal{T}_H\},$$

where \mathcal{T}_H is a partition of Ω in simplicial elements K of diameter H_K , and $\mathcal{P}^1(K)$ is the space of linear polynomials on K (quadrilateral elements could also be used, provided an adequate quadrature formula [2]). For each macro element, an approximation of the homogenized tensor on each integration point x_K is needed. Such approximation is obtained by solving a micro problem defined on the sampling domains $K_\delta = x_K + (-\delta/2, \delta/2)^d$, ($\delta \geq \varepsilon$). For a sampling domain K_δ we define a micro finite element space

$$(4.3) \quad S^1(K_\delta, \mathcal{T}_h) = \{z^h \in W(K_\delta) : z^h|_T \in \mathcal{P}^1(T) \forall T \in \mathcal{T}_h\}.$$

The space $W(K_\delta)$ is defined as

$$W(K_\delta) = W_{per}^1 = \{z \in H_{per}^1(K_\delta) : \int_{K_\delta} z \, dx = 0\}$$

in case we ask for periodic coupling, or

$$W(K_\delta) = H_0^1(K_\delta)$$

for a coupling with Dirichlet boundary conditions. We make the assumption of A^ε of being locally periodic and admitting explicit scale separation between slow and fast spatial variables, so that $A^\varepsilon(x) = A(x, x/\varepsilon)$. Let u^H be the approximate solution to the homogenized problem originating from (4.1). Then the numerical method is defined as follows: find $u^H \in S^1(\Omega, \mathcal{T}_H)$, $u^H = g$ on $\partial\Omega$, such that

$$B_H(u^H, v^H) = F_H(v^H) \quad \forall v^H \in S_0^1(\Omega, \mathcal{T}_H),$$

where

$$(4.4) \quad B_H(v^H, w^H) := \sum_{K \in \mathcal{T}_H} \frac{|K|}{|K_\delta|} \int_{K_\delta} A(x_K, x/\varepsilon) \nabla v_K^h \cdot \nabla w_K^h \, dx,$$

and

$$F_H(v^H) := \sum_{K \in \mathcal{T}_H} |K| (f v^H)(x_K).$$

In (4.4) v_K^h (respectively w_K^h) denotes the solution to the micro problem: find v_K^h such that $v_K^h - v^H \in S^1(K_\delta, \mathcal{T}_h)$ and

$$(4.5) \quad \int_{K_\delta} A^\varepsilon \nabla v_K^h \cdot \nabla z^h \, dx = 0 \quad \forall z^h \in S^1(K_\delta, \mathcal{T}_h).$$

We conclude this brief section by recalling the convergence estimates for the numerical method which have been extensively studied in the literature [1, 3]:

$$\begin{aligned} \|u^0 - u^H\|_{H^1(\Omega)} &\leq C \left(H^1 + \left(\frac{h}{\varepsilon}\right)^2 + e_{MOD} \right), \\ \|u^0 - u^H\|_{L^2(\Omega)} &\leq C \left(H^2 + \left(\frac{h}{\varepsilon}\right)^2 + e_{MOD} \right). \end{aligned}$$

Moreover for the homogenized tensor we have

$$\sup_{\substack{K \in \mathcal{T}_H \\ x \in K}} \|A^0(x) - A^{0,h}(x)\|_F \leq C \left(H^1 + \left(\frac{h}{\varepsilon}\right)^2 + e_{MOD} \right),$$

where $\|\cdot\|_F$ denotes the Frobenius norm and $A^{0,h}$ is defined in (4.17). The term e_{MOD} is the so called modelling error and does not depend on H and h . For locally periodic tensors which admit explicit separation between the slow and fast variable, if collocated at the slow variable, this term vanishes (see [1, 3]).

Remark. We emphasize that the method can be generalized for macro and micro finite element spaces of higher orders r and q respectively. Let \mathcal{T}_H be a simplicial mesh and $S_0^r(\Omega, \mathcal{T}_H)$ be the macro finite element space of polynomials of total degree r , and let $\{x_{K_p}, \omega_{K_p}\}_{p=1}^P$ a quadrature formula exact for polynomials in $\mathcal{P}^{r^*}(K)$, $r^* = \max\{2r-2, r\}$ (quadrilateral elements and polynomials of total degree at most r in each variable could also be used provided appropriate changes in the numerical quadrature formula). Then the homogenized tensor has to be computed for each quadrature point by solving micro problems on sampling domains K_{δ_p} . The bilinear form of the method becomes then

$$B_H(v^H, w^H) := \sum_{K \in \mathcal{T}_H} \sum_{p=1}^P \frac{\omega_{K_p}}{|K_{\delta_p}|} \int_{K_{\delta_p}} A(x_{K_p}, x/\varepsilon) \nabla v_{K_p}^h \cdot \nabla w_{K_p}^h \, dx,$$

where $v_{K_p}^h$ (respectively $w_{K_p}^h$) denotes the solution to the micro problem: find $v_{K_p}^h$ such that $v_{K_p}^h - v_{lin,p}^H \in S^q(K_{\delta_p}, \mathcal{T}_h)$ and

$$\int_{K_{\delta_p}} A^\varepsilon \nabla v_{K_p}^h \cdot \nabla z^h \, dx = 0 \quad \forall z^h \in S^q(K_{\delta_p}, \mathcal{T}_h),$$

where $v_{lin,p}^H := v^H(x_{K_p}) + (x - x_{K_p}) \cdot \nabla v^H(x_{K_p})$.

4.2. Approximate boundary flux calculations. Here we describe a numerical method to approximate the flux at the boundary. This method is based on a Galerkin projection, and is analysed in detail in [31] in its classical finite element formulation. In particular it allows to obtain superconvergence of the approximate flux

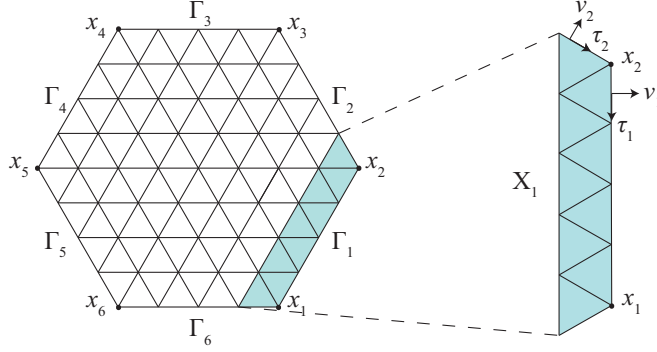


Figure 1: An example of a domain characterized by six edges and corners. On the right the strip of elements $X_1(\Omega, \mathcal{T}_H)$ is represented. On the corners the flux at the boundary is specified by the Dirichlet condition g .

in the $L^2(\partial\Omega)$ -norm, and we show how such superconvergence result can be extended in the context of FE-HMM. In what follows we assume Ω to be a polygonal domain, and $\partial\Omega = \cup_{j=1}^J \Gamma_j$, where Γ_j are the straight interface portions defining $\partial\Omega$. Since the normal flux at the corners of Ω is not well defined, we assume that the approximate flux at the corners is specified from direct calculations with the given Dirichlet condition. For example, for the case given in Figure 1, this direct calculation is performed as follows:

$$\begin{aligned} \nabla u \cdot \nu_2(x_2) &= \nabla g(x_2) \cdot (a\tau_2 + b\tau_1), \\ a &= (\nu_2 \cdot \nu_1) / (\tau_2 \cdot \nu_1), \quad b = 1 / (\tau_2 \cdot \nu_1). \end{aligned}$$

Finally the method aims at computing the normal flux at the boundary by considering one straight interface Γ_j at the time, so that the $\Lambda_{A^0} g = \{(\Lambda_{A^0} g)_j\}_{j=1}^J$, where

$$(\Lambda_{A^0} g)_j = A^0 \nabla u^0 \cdot \nu|_{\Gamma_j}.$$

Let us introduce the following subspaces of $S^1(\Omega, \mathcal{T}_H)$:

$$\begin{aligned} S_c^1(\Omega, \mathcal{T}_H) &= \{v^H \in S^1(\Omega, \mathcal{T}_H) : v^H = 0 \text{ at the corners of } \Omega\}, \\ S_i^1(\Omega, \mathcal{T}_H) &= \{v^H \in S^1(\Omega, \mathcal{T}_H) : v^H = 0 \text{ at the interior nodes of } \Omega\}. \end{aligned}$$

Let us denote as $S_0^1(\Gamma_j, \mathcal{T}_H)$, $j = 1, \dots, J$, the finite dimensional spaces of functions which are restrictions on the boundary portions Γ_j of functions in $S_c^1(\Omega, \mathcal{T}_H)$. Finally let $X_j(\Omega, \mathcal{T}_H)$ denote the strip of all the elements in \mathcal{T}_H , which have at least one vertex on Γ_j , $j = 1, \dots, J$. Using integration by parts we have the following relation for the flux

$$(4.6) \quad - \int_{\Gamma_j} (\Lambda_{A^0} g)_j \cdot v^H \, ds = B_j(u^0, v^H) - \int_{X_j} f v^H \, dx,$$

$\forall v^H \in S_c^1(\Omega, \mathcal{T}_H) \cap S_i^1(\Omega, \mathcal{T}_H)$, where

$$B_j(v, w) = \int_{X_j} A^0 \nabla v \cdot \nabla w \, dx.$$

Then following [12, 31] an approximate flux can be constructed by progressively assembling functions $(\Lambda_{A^0,h}^H g)_j \in S_0^1(\Gamma_j, \mathcal{T}_H)$, $j = 1, \dots, J$, such that

$$(4.7) \quad - \int_{\Gamma_j} (\Lambda_{A^0,h}^H g)_j \cdot v^H \, ds = B_{H,j}(u^H, v^H) - \int_{X_j} f v^H \, dx$$

$\forall v^H \in S_c^1(\Omega, \mathcal{T}_H) \cap S_i^1(\Omega, \mathcal{T}_H)$, where

$$B_{H,j}(v^H, w^H) = \sum_{K \in X_j} \frac{|K|}{|K_\delta|} \int_{K_\delta} A(x_K, x/\varepsilon) \nabla v_K^h \cdot w_K^h \, dx,$$

for each $j = 1, \dots, J$. Let us remark that u^H has been already computed, and so constructing $\{(\Lambda_{A^0,h}^H g)_j\}_{j=1}^J$ leads then to solving J linear system whose unknowns are the values of the flux on the interior nodes of each Γ_j . To obtain an error estimate for the approximate boundary flux we recall the following lemma which relates the functions in $S_i^1(\Omega, \mathcal{T}_H)$ and their traces on $\partial\Omega$.

LEMMA 4.1. *Let $X = X(\Omega, \mathcal{T}_H)$ denote a strip of elements in \mathcal{T}_H , with each element having at least one vertex on $\partial\Omega$, and let $v^H \in S_i^1(\Omega, \mathcal{T}_H)$. Then*

$$\|\nabla v^H\|_{L^2(X)} \leq CH^{-1/2} \|v^H\|_{L^2(\partial\Omega)}.$$

Let $\mathcal{I}^H(\Lambda_{A^0} g)_j$ be the linear interpolation of $(\Lambda_{A^0} g)_j$ on Γ_j .

LEMMA 4.2. *The following interpolation error estimate holds:*

$$\langle (\Lambda_{A^0} g)_j - \mathcal{I}^H(\Lambda_{A^0} g)_j, v^H \rangle_{L^2(\Gamma_j), L^2(\Gamma_j)} \leq CH^{3/2} \|u^0\|_{H^3(\Omega)} \|v^H\|_{L^2(\Gamma_j)}.$$

Proof. The proof is given in [31], and it is a consequence of the Bramble-Hilbert lemma. \square

Following [31] we can then obtain the following theorem which establishes high order convergence to zero of the error for the approximate flux in the $L^2(\partial\Omega)$ -norm.

THEOREM 4.3. *Consider a quasi-uniform family of macroscopic triangulations $\{\mathcal{T}_H\}_{H>0}$. Assume that the coupling between macro and micro meshes follows $H = \mathcal{O}(h/\varepsilon)$. Let the solution u^0 of the effective problem be in $H^3(\Omega)$ and the coefficients $a_{ij}^0 \in W^{2,\infty}(\Omega)$. Then the approximate boundary flux computed by means of (4.7) satisfies*

$$\|\Lambda_{A^0} g - \Lambda_{A^0,h}^H g\|_{L^2(\partial\Omega)} = \left(\sum_{j=1}^J \|(\Lambda_{A^0} g)_j - (\Lambda_{A^0,h}^H g)_j\|_{L^2(\Gamma_j)}^2 \right)^{1/2} \leq C \left(H^{3/2} + \left(\frac{h}{\varepsilon} \right)^{3/2} \right),$$

where C is a constant independent on H , h , and ε .

Proof. Subtracting (4.7) from (4.6) we obtain, for $j = 1, \dots, J$,

$$(4.8) \quad \langle (\Lambda_{A^0} g)_j - (\Lambda_{A^0,h}^H g)_j, v^H \rangle_{L^2(\Gamma_j), L^2(\Gamma_j)} = B_j(u^0, v^H) - B_{H,j}(u^H, v^H)$$

$\forall v^H \in S_c^1(\Omega, \mathcal{T}_H) \cap S_i^1(\Omega, \mathcal{T}_H)$. Next we define the bilinear forms

$$B_{H,j}^0(v^H, w^H) := \sum_{K \in X_j} |K| \int_K A^0(x_K) \nabla v_K^H \cdot \nabla w_K^H \, dx,$$

and

$$\tilde{B}_H(v^H, w^H) := \sum_{K \in X_j} \frac{K}{|K_\delta|} \int_{K_\delta} A(x_K, x/\varepsilon) \nabla v_K \cdot \nabla w_K \, dx,$$

where v_K, w_K are the exact solutions to the micro problem (4.5) in the space of functions $W(K_\delta)$. Hence (4.8) can be estimated by

$$\begin{aligned} \langle (\Lambda_{A^0} g)_j - (\Lambda_{A^{0,h}}^H g)_j, v^H \rangle_{L^2(\Gamma_j), L^2(\Gamma_j)} &\leq \underbrace{|B_j(u^0, v^H) - B_{H,j}^0(\mathcal{I}^H u^0, v^H)|}_{I_1} \\ &\quad + \underbrace{|B_{H,j}^0(\mathcal{I}^H u^0, v^H) - \tilde{B}_{H,j}(u^H, v^H)|}_{I_2} \\ &\quad + \underbrace{|\tilde{B}_{H,j}(u^H, v^H) - B_{H,j}(u^H, v^H)|}_{I_3}, \end{aligned}$$

where \mathcal{I}^H denotes the linear interpolation operator. From [31] it follows that

$$I_1 \leq CH^2(\|u^0\|_{H^3(\Omega)} + \|f\|_{H^2(\Omega)}) \|\nabla v^H\|_{L^2(X_j)}.$$

On the other hand, it is well known [1, 3] that

$$I_3 \leq C \left(\frac{h}{\varepsilon} \right)^2 \|\nabla u^H\|_{L^2(\Omega)} \|\nabla v^H\|_{L^2(X_j)},$$

where C is a constant which is independent of δ and x_K . The term I_2 captures the modelling error, which vanishes under the assumption that the locally periodic tensor admits explicit separation between slow and fast variables, and it is collocated at the slow variable. Hence from Lemma 4.1 we get that

$$\langle (\Lambda_{A^0} g)_j - (\Lambda_{A^{0,h}}^H g)_j, v^H \rangle_{L^2(\Gamma_j), L^2(\Gamma_j)} \leq C \left(H^{3/2} + \left(\frac{h}{\varepsilon} \right)^2 H^{-1/2} \right) \|v^H\|_{L^2(\partial\Omega)}.$$

Then we choose

$$v^H = \begin{cases} \mathcal{I}^H(\Lambda_{A^0} g)_j - (\Lambda_{A^{0,h}}^H g)_j & \text{on } \Gamma_j, \\ 0 & \text{on } \partial\Omega \setminus \Gamma_j, \end{cases}$$

where \mathcal{I}^H is the linear interpolation operator that appears in Lemma 4.2. Hence, from the triangle inequality we obtain

$$\|(\Lambda_{A^0} g)_j - (\Lambda_{A^{0,h}}^H g)_j\|_{L^2(\Gamma_j)} \leq C \left(H^{3/2} + \left(\frac{h}{\varepsilon} \right)^2 H^{-1/2} \right),$$

for $j = 1, \dots, J$. Now, for $H = \mathcal{O}(h/\varepsilon)$ we can finally conclude that

$$(4.9) \quad \|(\Lambda_{A^0} g)_j - (\Lambda_{A^{0,h}}^H g)_j\|_{L^2(\Gamma_j)} \leq C \left(H^{3/2} + \left(\frac{h}{\varepsilon} \right)^{3/2} \right),$$

for each $j = 1, \dots, J$, and the desired assertion immediately follows. \square

Remark. Let us note that for a given accuracy, the computational cost for solving the micro problems is independent of ε , since the size of the micro domain $\delta \geq \varepsilon$ is proportional to ε . Let N_{mac} and N_{mic} be the degrees of freedom in one direction for the macro domain and the micro domain respectively. Then (4.9) can be rewritten as

$$(4.10) \quad \|(\Lambda_{A^0} g)_j - (\Lambda_{A^{0,h}}^H g)_j\|_{L^2(\Gamma_j)} \leq C \left(N_{mac}^{-3/2} + N_{mic}^{-3/2} \right),$$

for each $j = 1, \dots, J$. Hence, by choosing $N_{mac} = N_{mic} = N$ for optimal convergence, the total complexity is $\mathcal{O}(N^{2d})$ for an accuracy of $\mathcal{O}(N^{-3/2})$. Finally we emphasize that the micro problems are independent one from another and can be solved in parallel. Hence the complexity of the method can be further reduced.

We perform some numerical experiments to test the convergence of the method and to observe how the micro error affects the approximate flux. We consider the elliptic problem

$$\begin{aligned} -\nabla \cdot (A^\varepsilon \nabla u^\varepsilon) &= 0 && \text{in } \Omega, \\ u^\varepsilon &= g && \text{on } \partial\Omega. \end{aligned}$$

The domain Ω is defined as

$$\Omega = \{x = (x_1, x_2) : 0 < x_1, x_2 < 1\},$$

while

$$g = \sin(\pi(x_1 + x_2)).$$

We perform two numerical tests for two different choices of A^ε . In the first experiment we consider

$$\begin{aligned} a_{11}(x, x/\varepsilon) &= (16(x_1^2 - x_1)(x_2^2 - x_2) + 1)(\cos^2\left(2\pi\frac{x_1}{\varepsilon}\right) + 1), \\ a_{22}(x, x/\varepsilon) &= (16(x_1^2 - x_1)(x_2^2 - x_2) + 1)(\sin\left(2\pi\frac{x_2}{\varepsilon}\right) + 2), \\ a_{12}(x, x/\varepsilon) &= a_{21}(x, x/\varepsilon) = 0. \end{aligned}$$

We compute the approximate flux on the boundary nodes by means of the FE-HMM. We solve the problem for different choices of H and h/ε . To compute the error we use as reference solution the one obtained with $H = h/\varepsilon = 1/64$. The size of the micro domain is such that $\delta = \varepsilon$. Numerical results are shown in Table 1 and Figure 2.

	$H = 1/4$	$H = 1/8$	$H = 1/16$	$H = 1/32$	$H = 1/64$
$h/\varepsilon = 1/4$	2.304	0.8864	0.5373	0.4643	0.4485
$h/\varepsilon = 1/8$	1.9243	0.5417	0.1601	0.0658	0.0469
$h/\varepsilon = 1/16$	1.8896	0.5140	0.1328	0.0331	0.0093
$h/\varepsilon = 1/32$	1.8827	0.5087	0.1280	0.0281	0.0019
$h/\varepsilon = 1/64$	1.8810	0.5074	0.1269	0.0270	

Table 1: First experiment, error $\|\Lambda_{A^0} g - \Lambda_{A^{0,h}}^H g\|_{L^2(\partial\Omega)}$ for different choices of H and h/ε ($\delta = \varepsilon$).

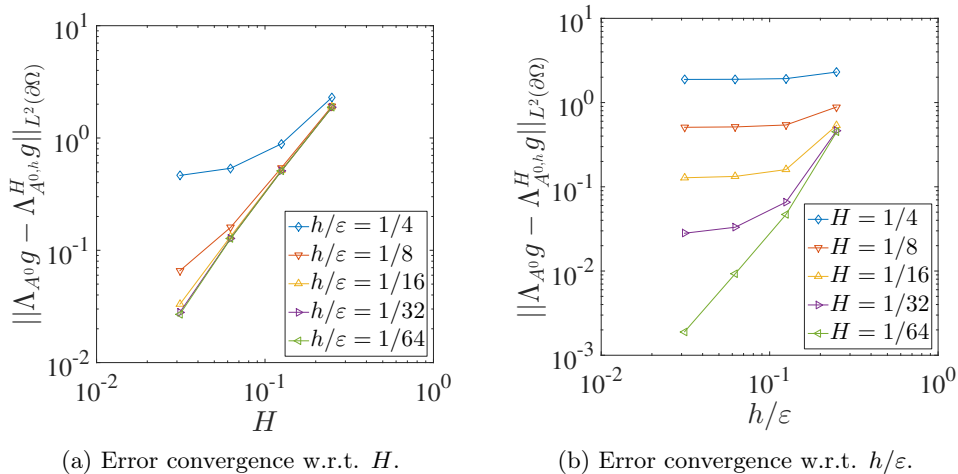


Figure 2: First experiment, convergence of the error $\|\Lambda_{A^0}g - \Lambda_{A^0,h}^H g\|_{L^2(\partial\Omega)}$ ($\delta = \varepsilon$).

In the second experiment we consider the tensor

$$\begin{aligned}
 a_{11}(x, x/\varepsilon) &= \left(\sqrt{\left(x_1^2 + \sin\left(2\pi\frac{x_1}{\varepsilon}\right) + 1.2\right) \left(x_1x_2 + \sin\left(4\pi\frac{x_1}{\varepsilon}\right) + 1.5\right)} \right)^{-1}, \\
 a_{22}(x, x/\varepsilon) &= \left(\left(x_1x_2 + \sin\left(5\pi\frac{x_2}{\varepsilon}\right) + 1.2\right) \left(x_2^2 \cos\left(2\pi\frac{x_2}{\varepsilon}\right) + x_1 + 1.5\right) \right)^{-1}, \\
 a_{12}(x, x/\varepsilon) &= a_{21}(x, x/\varepsilon) = 0.
 \end{aligned}$$

As shown in Table 1, 2 and Figure 2, 3, the error converges quadratically as we decrease both H and h/ε . In particular for the problems considered the global error seems to depend more on the macro mesh. For the micro error we can observe quadratic convergence only for smaller values of H , while for bigger values the micro error convergence saturates due to the dominant macro error. Finally let us mention that the quadratic convergence has been observed also in [12] for the FEM formulation of the method, suggesting that the error estimate obtained in [31] may not be sharp.

	$H = 1/4$	$H = 1/8$	$H = 1/16$	$H = 1/32$	$H = 1/64$
$h/\varepsilon = 1/4$	0.4317	0.1508	0.0910	0.0845	0.0841
$h/\varepsilon = 1/8$	0.3975	0.1175	0.0400	0.0243	0.0222
$h/\varepsilon = 1/16$	0.3879	0.1107	0.0316	0.0117	0.0080
$h/\varepsilon = 1/32$	0.3843	0.1085	0.0294	0.0079	0.0016
$h/\varepsilon = 1/64$	0.3834	0.1079	0.0290	0.0076	

Table 2: Second experiment, error $\|\Lambda_{A^0}g - \Lambda_{A^0,h}^H g\|_{L^2(\partial\Omega)}$ for different choices of H and h/ε ($\delta = \varepsilon$).

4.3. Solving the discrete inverse problem. We consider the discrete inverse problem regularized by means of the Tikhonov method introduced in Section 3. To solve the inverse problem numerically we discretize the domain by using

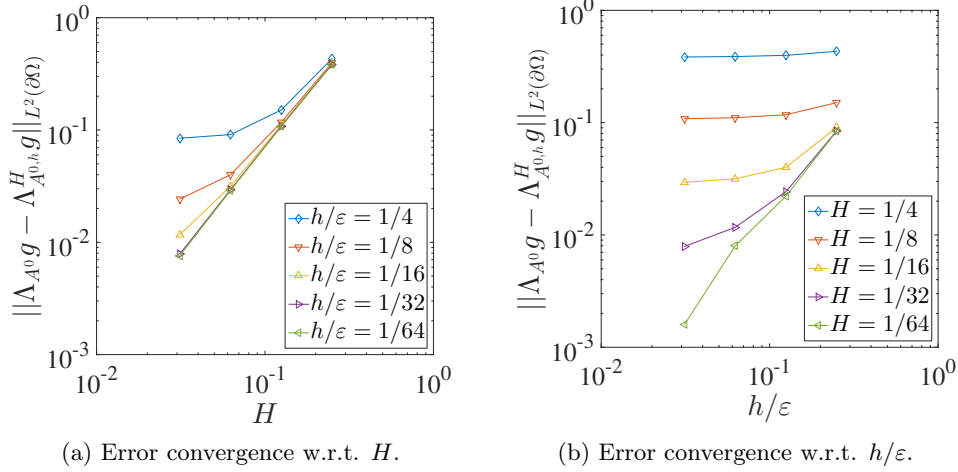


Figure 3: Second experiment, convergence of the error $\|\Lambda_{A^0}g - \Lambda_{A^0,h}^H g\|_{L^2(\partial\Omega)}$ ($\delta = \varepsilon$).

simplicial elements, and we approximate both the macro and micro finite element spaces with linear piecewise polynomials. Let us consider a locally periodic tensor $A^\varepsilon(x) = A(\sigma^*(x), x/\varepsilon)$. Input parameters to solve the problem are the set of boundary fluxes

$$(4.11) \quad \Lambda_{A(\sigma^*, x/\varepsilon)} g_l, \quad l = 1, \dots, L,$$

the range for the unknown $[\sigma^-, \sigma^+]$, and the matrix function $(t, y) \mapsto A(t, y)$, $t \in [\sigma^-, \sigma^+]$, $y = x/\varepsilon \in (0, 1)^d$. Next we define the discrete admissible set for the solution

$$U^H = \{\sigma^H \in S^1(\Omega, \mathcal{T}_H) : \sigma^- \leq \sigma^H \leq \sigma^+\}.$$

The discrete minimization problem reads: find $\bar{\sigma}^{\varepsilon, H} \in U^H$ such that

$$(4.12) \quad \Psi_{H,h}^\varepsilon(\bar{\sigma}^{\varepsilon, H}) = \inf_{\sigma^H \in U^H} \Psi_{H,h}^\varepsilon(\sigma^H)$$

where

$$\begin{aligned} \Psi_{H,h}^\varepsilon(\sigma^H) &= \sum_{l=1}^L \|\Lambda_{A(\sigma^*, x/\varepsilon)} g_l - \Lambda_{A^0,h(\sigma^H)}^H g_l\|_{L^2(\partial\Omega)}^2 + \gamma \|\sigma^H - \sigma_0\|_{H^1(\Omega)}^2 \\ &= \Phi_{H,h}^\varepsilon(\sigma^H) + \gamma \|\sigma^H - \sigma_0\|_{H^1(\Omega)}^2. \end{aligned}$$

The minimization problem is solved by means of the interior point algorithm (for example see [10] for details). For each new admissible guess $\sigma^H \in U^H$ and for each $l = 1, \dots, L$ we compute the approximate boundary flux by solving for each Γ_j , $j = 1, \dots, J$, $\partial\Omega = \cup_{j=1}^J \Gamma_j$, the linear system

$$-\int_{\Gamma_j} (\Lambda_{A^0,h(\sigma^H)}^H g_l)_j \cdot v^H \, ds = B_{H,j}(u^H, v^H) \quad \forall v^H \in S_c^1(\Omega, \mathcal{T}_H) \cap S_i^1(\Omega, \mathcal{T}_H),$$

with

$$B_{H,j}(v^H, w^H) = \sum_{K \in X_j} \frac{|K|}{|K_\delta|} \int_{K_\delta} A(\sigma^H(x_K), x/\varepsilon) \nabla v_K^h \cdot w_K^h dx.$$

When $\Psi_{H,h}^\varepsilon$ does not decrease any more, or the gradient of the objective function decreases under a certain tolerance that we choose a priori, the minimization process stops. The set U^H is finite dimensional and uniformly bounded. Thus the existence of a minimizer $\bar{\sigma}^{\varepsilon,H} \in U^H$ to the discrete optimization problem (4.12) is ensured for any $H > 0$ by compactness and norm equivalence of finite dimensional spaces. One question we would like to answer to, is whether the sequence $\{\bar{\sigma}^{\varepsilon,H}\}_{H>0}$ of discrete solutions converges to a minimizer $\bar{\sigma}^\varepsilon$ of the continuous problem as we refine the mesh. To this end we first state a discrete analogue of Lemma 3.1.

LEMMA 4.4. *Suppose the assumptions of Theorem 4.3 hold, and let the sequence $\{\sigma^H\}_{H>0} \in U^H \subset U$ converges in $L^r(\Omega)$, $r \geq 1$, to some $\sigma \in U$ as H tends to zero. The the sequence of approximations $\{\Lambda_{A^0,h(\sigma_H)}^H g\}_{H>0}$ converges to $\Lambda_{A^0(\sigma)} g$ in $L^2(\partial\Omega)$ as H, h tend to zero.*

Proof. The desired assertion easily follows from Lemma 3.1 and the estimate (4.9). \square

Now, thanks to Lemma 4.4 we can state the convergence of the discrete approximate solutions $\{\bar{\sigma}^{\varepsilon,H}\}_{H>0}$. Let $\bar{\sigma}^\varepsilon$ be a solution of the regularized inverse problem in the infinite dimension, so that

$$(4.13) \quad \Psi^\varepsilon(\bar{\sigma}^\varepsilon) = \inf_{\sigma \in U} \Psi^\varepsilon(\sigma),$$

where

$$\begin{aligned} \Psi^\varepsilon(\sigma) &= \sum_{l=1}^L \|\Lambda_{A(\sigma^*, x/\varepsilon)} g_l - \Lambda_{A^0(\sigma)} g_l\|_{L^2(\partial\Omega)}^2 + \gamma \|\sigma - \sigma_0\|_{H^1(\Omega)}^2 \\ &= \Phi^\varepsilon(\sigma) + \gamma \|\sigma - \sigma_0\|_{H^1(\Omega)}^2. \end{aligned}$$

THEOREM 4.5. *Suppose the assumptions of Theorem 4.3 hold, and consider the sequence of minimization problems of type (4.12) for $H, h \rightarrow 0$. The sequence of minimizers $\{\bar{\sigma}^{\varepsilon,H}\}_{H>0}$ contains a subsequence that converges weakly in $H^1(\Omega)$ to a minimizer $\bar{\sigma}^\varepsilon$ of problem (4.13) as $H, h \rightarrow 0$.*

Proof. Our proof is inspired from [21]. Here we briefly sketch the main steps to obtain the desired result. Let $\mathcal{I}^H := U \rightarrow U^H$ be the linear interpolation operator. We start by noting that the minimizing properties of $\{\bar{\sigma}^{\varepsilon,H}\}_{H>0}$ imply that for each $H, h > 0$, $\Psi_{H,h}^\varepsilon(\bar{\sigma}^{\varepsilon,H})$ is bounded by $\Psi_{H,h}^\varepsilon(\mathcal{I}^H \bar{\sigma}^\varepsilon)$, which is in turn bounded with respect to H and h . Then $\{\bar{\sigma}^{\varepsilon,H}\}_{H>0}$ admits a subsequence $\{\bar{\sigma}^{\varepsilon,H'}\}_{H'>0}$ which weakly converges to some $\bar{\sigma}^\varepsilon$ in $H^1(\Omega)$. Then from Lemma 4.4 and weak lower semi-continuity of the $H^1(\Omega)$ -norm we get that

$$\Psi^\varepsilon(\bar{\sigma}^\varepsilon) \leq \liminf_{H,h \rightarrow 0} \Psi_{H,h}^\varepsilon(\bar{\sigma}^{\varepsilon,H}).$$

It remains now to show that $\bar{\sigma}^\varepsilon$ is indeed the minimizer of problem (4.13). Since $C^\infty(\bar{\Omega})$ is dense in $H^1(\Omega)$, we have that for any $\sigma \in U$, there exists a sequence $\{\sigma_n\}_{n>0} \in C^\infty(\bar{\Omega}) \cap U$ such that

$$(4.14) \quad \lim_{n \rightarrow \infty} \|\sigma_n - \sigma\|_{H^1(\Omega)} = 0.$$

The minimizing properties of $\{\bar{\sigma}^{\varepsilon, H}\}_{H>0}$ imply that

$$\Psi_{H,h}^{\varepsilon}(\bar{\sigma}^{\varepsilon, H}) \leq \Psi_{H,h}^{\varepsilon}(\mathcal{I}^H \sigma_n) \quad \forall n > 0.$$

Letting $H, h/\varepsilon \rightarrow 0$, we obtain from the approximation properties of \mathcal{I}^H , Lemma 4.4, and (4.3), that

$$\Psi^{\varepsilon}(\bar{\sigma}^{\varepsilon}) \leq \Psi^{\varepsilon}(\sigma_n) \quad \forall n > 0.$$

Since σ is arbitrary, by letting $n \rightarrow \infty$, we deduce from (4.14) and Lemma 3.1 that

$$\Psi^{\varepsilon}(\bar{\sigma}^{\varepsilon}) \leq \Psi^{\varepsilon}(\sigma) \quad \forall \sigma \in U,$$

and the desired assertion follows. \square

4.4. Model order reduction. The FE-HMM, as it is defined, can result in being computationally expensive, since it requires the computation of a cell problem for each macro element and each macro quadrature point, whose number increases as we refine the macro mesh for an appropriate approximation of the homogenized solution. This is particularly undesirable when solving inverse problems, since typically one needs multiple evaluations of the cost functional for different guesses of the parameter of interest. Here we explain how reduced basis methodology can be combined with FE-HMM to design a new efficient method which drastically reduces the computational effort, by avoiding the repeated solutions of a large number of cell problems. For a detailed description and analysis of the method, called the Reduced Basis Finite Element Heterogeneous Multiscale Method (RB-FE-HMM), we mention [4]. The main idea is the following: instead of computing the micro solutions in each macro element at the given macro quadrature points, during what is called the *offline stage* we select a small number of carefully precomputed micro solutions to construct a small subspace of micro functions. Then in the *online stage* each micro solution is obtained as linear combination of the precomputed micro functions. The construction of the subspace is performed using a greedy procedure, and therefore a cheap way to compute residuals, in order to have efficiency of the a posteriori error control, is crucial. Assume $A^{\varepsilon}(x) = A(\sigma(x), x/\varepsilon)$ being locally periodic and admitting scale separation between slow and fast variables. We start with the following reformulation of the FE-HMM, which makes a link between the micro problems and the effective tensor:

$$(4.15) \quad \frac{1}{|K_{\delta}|} \int_{K_{\delta}} A(\sigma(x_K), x/\varepsilon) \nabla v_K^h \cdot \nabla w_K^h \, dx = A^{0,h}(\sigma(x_K)) \nabla v^H(x_K) \cdot \nabla w^H(x_K).$$

We map the domain K_{δ} into the reference domain $Y = (0, 1)^d$ through $x = G_{x_K}(y) = x_K + \delta(y - 1/2)$. Then we obtain

$$(4.16) \quad B_H(v^H, w^H) := \sum_{K \in \mathcal{T}_H} |K| A^{0,h}(\sigma(x_K)) \nabla v^H(x_K) \cdot \nabla w^H(x_K),$$

where

$$(4.17) \quad (A^{0,h}(\sigma(x_K)))_{ik} = \int_Y A_{x_K}(\nabla \chi_K^{i,h} + \mathbf{e}_i) \cdot (\nabla \chi_K^{k,h} + \mathbf{e}_k) \, dy,$$

where $A_{x_K} = A(\sigma(x_K), G_{x_K}(y))$. Finally $\chi_K^{i,h}$ (respectively $\chi_K^{k,h}$) is the solution of the micro problem

$$(4.18) \quad \begin{aligned} b(\chi_K^{i,h}, z^h) &:= \int_Y A_{x_K} \nabla \chi_K^{i,h} \cdot \nabla z^h \, dy \\ &= - \int_Y A_{x_K} \mathbf{e}_i \cdot \nabla z^h \, dy =: l_i(z^h) \quad \forall z^h \in S^1(Y, \mathcal{T}_h). \end{aligned}$$

In the offline stage we construct a reduced space of N carefully precomputed micro solutions, which we call $S_N(Y)$. Details on how the procedure is carried on can be found in [4]. To select the basis functions a greedy algorithm is used. We start by randomly defining the training set $\Xi_{Train} = \{(t_n, \eta_n) : 1 \leq n \leq N_{Train}, 1 \leq \eta_n \leq d\}$, where $t_n \in [\sigma^-, \sigma^+]$, while η_n corresponds to the unit vector \mathbf{e}_{η_n} of the canonical basis of \mathbb{R}^d . We compute the first basis function ζ_1^h and initialize the reduced space $S_N(Y)$. Then, successively we continue to add new basis functions to $S_N(Y)$ until convergence of the a posteriori error is detected. A crucial assumption to efficiently evaluate the a posteriori error is that, for a given $t_n \in [\sigma^-, \sigma^+]$, the tensor $A(t_n, y)$ is available in the affine form

$$(4.19) \quad A(t_n, y) = \sum_{m=1}^M \Theta_m(t_n) A_m(y), \quad \forall y \in Y.$$

However in the case $A(t_n, y)$ is not directly available in the form (4.19), a greedy algorithm, called the empirical interpolation method (EIM), can be applied to obtain an affine approximation of $A(t_n, y)$ [22]. The output of the offline stage is the reduced space

$$S_N(Y) = \text{span}\{\zeta_1^h, \dots, \zeta_N^h\}.$$

Then we define a macro method similar to FE-HMM, with micro functions computed on the reduced space. The method reads: find $u^{H, RB} \in S^1(\Omega, \mathcal{T}_H)$, $u^{H, RB} = g$ on $\partial\Omega$, such that

$$B_{H, RB}(u^{H, RB}, v^H) = \int_{\Omega} f v^H \, dx \quad \forall v^H \in S_0^1(\Omega, \mathcal{T}_H),$$

where

$$(4.20) \quad B_{H, RB}(v^H, w^H) := \sum_{K \in \mathcal{T}_H} |K| A^{0, N}(x_K) \nabla v^H(x_K) \cdot w^H(x_K),$$

where

$$(A^{0, N}(x_K))_{ik} = \int_Y A_{x_K} (\nabla \chi_K^{i, N} + \mathbf{e}_i) \cdot (\nabla \chi_K^{k, N} + \mathbf{e}_k) \, dy,$$

where $\chi_K^{i, N}$ is the solution of (4.18) in the reduced basis space. Thanks to the affine representation of the tensor A^ε , solving the micro problems in the reduced space consists with solving an $N \times N$ linear system, which leads to a great saving of computational effort. Then we will denote the normal flux at the boundary obtained by

means of RB-FE-HMM as $\Lambda_{A^0, N}^H g$, where N stands for the dimension of the reduced space of micro functions.

Remark. Convergence results established in Section 4.3 still holds. In the convergence analysis we need to take into account the error due to the model order reduction. This error is based on the distance between the reduced space $S_N(Y)$ and $S^1(Y, \mathcal{T}_h)$. Such distance can be quantified by means of the notion Kolmogorov N -width (see [4]).

5. Numerical experiments. In this section we present numerical experiments that illustrate the behaviour of the proposed numerical method for solving inverse problems. We first explain how we define the Dirichlet conditions $\{g_l\}_{l=1}^L$ and how we collect multiscale observations. Then we solve the inverse problem for two different types of macroscopic parametrizations: an affine parametrization which controls the amplitude of the micro oscillations characterizing A^ε , and a non-affine parametrization controlling their orientation. In particular for the first parametrization, we perform different numerical tests to observe the sensitivity of the results with respect to the several parameters involved (γ , ε , H , L) and assess our theoretical findings. For the second parametrization we fix the values of such parameters and we report the solution obtained by means of the proposed algorithm for solving multiscale inverse problems. To conclude we remark that the forward homogenized problem is computed by means of RB-FE-HMM, and the offline stage is performed for the following choice of the parameters: $h/\varepsilon = 1/64$, $\delta = \varepsilon$, $tol_{RB} = 10^{-11}$, where tol_{RB} is the prescribed tolerance used as stopping criterion for the greedy process we use to select the micro basis function.

5.1. Set-up. The set up of the numerical experiments is as follows. The domain Ω is defined as

$$\Omega = \{x = (x_1, x_2) : 0 < x_1, x_2 < 1\}.$$

We compute then the multiscale fluxes $\Lambda_{A^\varepsilon}^{h_{obs}} g_l$ for different Dirichlet conditions $\{g_l\}_{l=1}^L$ by means of FEMs, using a mesh size $h_{obs} \ll \varepsilon$. In particular we take $\{g_l\}_{l=1}^L = \{\sqrt{\lambda_l} \varphi_l\}_{l=1}^L$, where $\{(\lambda_l, \varphi_l)\}_{l=1}^L$ are the L eigenpairs corresponding to the largest L eigenvalues of the one dimensional discrete Laplacian operator. Each g_l is then interpolated on the boundary $\partial\Omega$ to define the respective Dirichlet condition. This procedure ensures that the functions $\{g_l\}_{l=1}^L$ are smooth and orthonormal, so that each contribution is independent from the others. Moreover $\|\nabla g_l\|_{L^2(\partial\Omega)} < C$ where C is a constant independent of L . In Figure 4 the first five g_l functions are shown.

5.2. 2D affine parametrization. For the first parametrization we consider a tensor A^ε given by

$$\begin{aligned} a_{11}(\sigma^*(x), x/\varepsilon) &= \sigma^*(x) \left(\cos^2 \left(2\pi \frac{x_1}{\varepsilon} \right) + 1 \right) + \cos^2 \left(2\pi \frac{x_2}{\varepsilon} \right), \\ a_{22}(\sigma^*(x), x/\varepsilon) &= \sigma^*(x) \left(\sin \left(2\pi \frac{x_2}{\varepsilon} \right) + 2 \right) + \cos^2 \left(2\pi \frac{x_1}{\varepsilon} \right), \\ a_{12}(\sigma^*(x), x/\varepsilon) &= a_{21}(\sigma^*(x), x/\varepsilon) = 0, \end{aligned}$$

where

$$\sigma^*(x) = 16(x_1^2 - x_1)(x_2^2 - x_2) + 1.$$

For this first set of numerical experiments σ^* is a simple smooth parabola, and its profile together with the one of $A^\varepsilon(x)$ is shown in Figure 5.

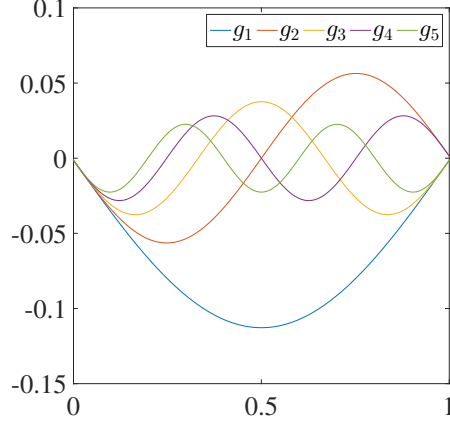


Figure 4: First five Dirichlet conditions used for the numerical experiments.

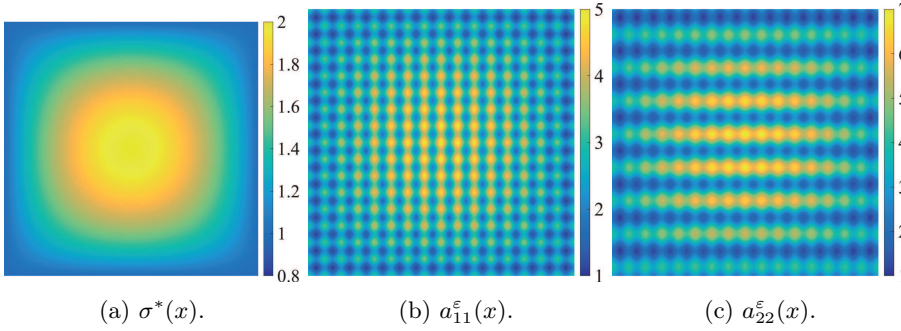


Figure 5: The true field σ^* and the two components a_{11}^ε and a_{22}^ε of the multiscale tensor ($\varepsilon = 1/8$).

Sensitivity with respect to γ . We start by observing how the solution to the problem

$$\begin{aligned} \Psi_{H,N}^\varepsilon(\bar{\sigma}^{\varepsilon,H}) &= \inf_{\sigma^H \in U^H} \Psi_{H,N}^\varepsilon(\sigma^H) \\ &= \inf_{\sigma^H \in U^H} \sum_{l=1}^L \|\Lambda_{A(\sigma^*,x/\varepsilon)}^{h_{obs}} g_l - \mathcal{I}^{h_{obs}} \Lambda_{A^{0,N}(\sigma^H)}^H g_l\|_{L^2(\partial\Omega)}^2 + \gamma \|\sigma^H - \sigma_0\|_{H^1(\Omega)}^2, \end{aligned}$$

behaves as we vary the regularization parameter γ , where $\mathcal{I}^{h_{obs}} \Lambda_{A^{0,N}(\sigma^H)}^H g_l$ is the linear extension of $\Lambda_{A^{0,N}(\sigma^H)}^H g_l$ on $S^1(\partial\Omega, \mathcal{T}_{h_{obs}})$. We set $\sigma_0 = 1$, while σ^- and σ^+ are chosen to be equal to 0.5 and 2.5 respectively. We fix $\varepsilon = 1/64$, $H = 1/16$, $L = 20$, and we solve the problem for different values of γ . The optimization problem is solved by means of the interior point method, with initial guess equal to σ_0 . The relative error we obtain is shown in Figure 6 for different norms and different values of γ . As can be observed, the approximated solutions we obtain, have different properties

which vary with the regularization parameter γ . The larger γ , the more regularized is the inverse problem. Thus, if γ is too large the solution is too regularized, and it can be far from the true scalar field we want to retrieve. On the other hand when γ becomes too small, the problem becomes more unstable, and much more oscillations are allowed in the reconstructed scalar field. For our problem we observe that the L^2 -error is minimum when $\gamma \in [2.5 \times 10^{-4}, 5 \times 10^{-4}]$.

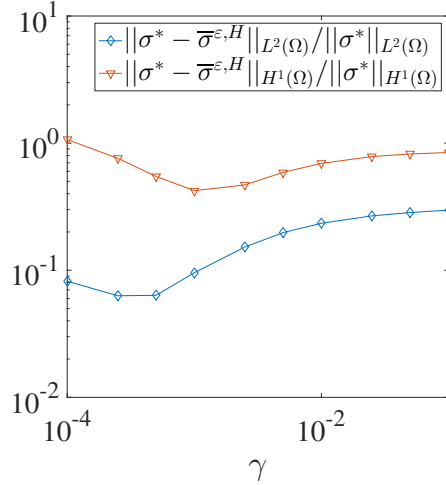


Figure 6: Error behaviour with respect to the regularization parameter γ .

Convergence with respect to ε . In this other numerical test we set $\gamma = 5 \times 10^{-4}$, and we verify the statement of Theorem 3.4. Moreover we check the convergence of the approximated solution towards $\bar{\sigma}^{0, H}$, which is the approximated solution of the discrete version of problem (3.4). Others parameters such as H and L are the same as in the previous numerical test. From Figure 7 we can see that the error $|\Psi_{H, N}^0(\bar{\sigma}^{0, H}) - \Psi_{H, N}^0(\bar{\sigma}^{\varepsilon, H})|$ converges to zero as $\varepsilon \rightarrow 0$, as expected from Theorem 3.4. Relative errors between $\bar{\sigma}^{0, H}$ and $\bar{\sigma}^{\varepsilon, H}$ are also shown in Figure 7 for both L^2 and H^1 norms. We can observe convergence of $\bar{\sigma}^{\varepsilon, H}$ to $\bar{\sigma}^{0, H}$ as $\varepsilon \rightarrow 0$, in agreement with Theorem 3.4. For relatively large values of ε , namely $\varepsilon > H$, the error we obtain is relatively large and no convergence is observed. This is due to the fact that, since $\varepsilon > H$, the approximate homogenized flux, which approximates at best the multiscale flux, is capable of capturing its typical oscillations. Hence, such oscillations will affect the retrieved solution as well.

Convergence with respect to H . To verify convergence with respect to discretization, we fix $\gamma = 5 \times 10^{-4}$, $\varepsilon = 1/64$, $L = 20$, and use the discrete minimizer $\bar{\sigma}^{\varepsilon, H}$ obtained on the finest discretization as reference solution. In Figure 8 we show the numerical errors obtained, and the picture agrees with what stated in Theorem 4.5.

Sensitivity with respect to L . Finally we let vary the number L of different Dirichlet conditions used to define the inverse problem, and check if a larger value of L leads to a better approximated solution. For this experiment $\gamma = 5 \times 10^{-4}$, $\varepsilon = 1/64$, $H = 1/16$, while we let vary L between 1 and 20. We can observe in Figure 9 that

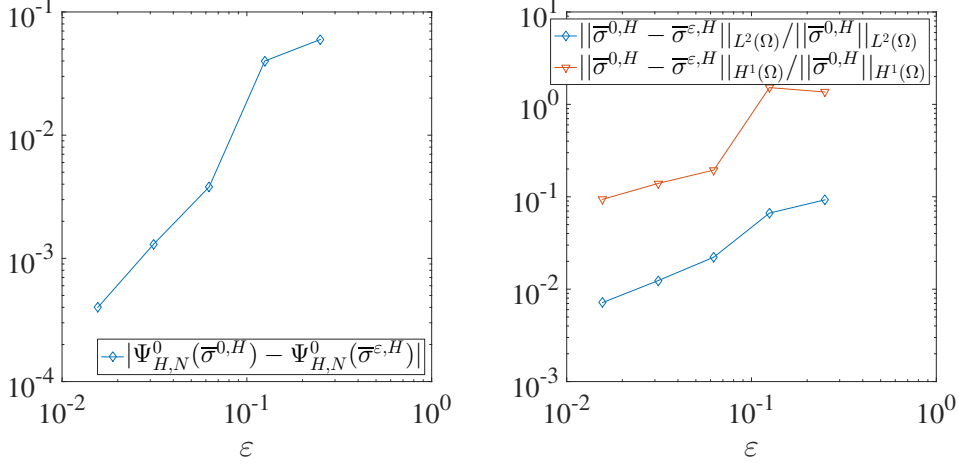


Figure 7: Error convergence as $\varepsilon \rightarrow 0$.

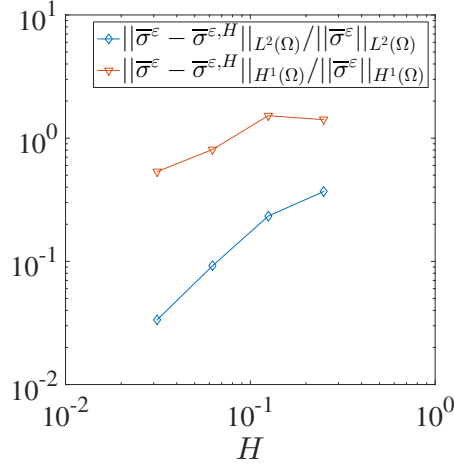


Figure 8: Error convergence as $H \rightarrow 0$.

the relative error between the exact function σ^* and our approximation decreases as L becomes larger. However it is also important to mention that as L increases, we should decrease H since the functions g_l becomes more and more oscillating as $L \rightarrow \infty$, and therefore we need a small mesh size to approximate them well. This could be also the reason why the H^1 -error increases for the last larger values of L .

Finally in Figure 10 we show the conductivity tensor we retrieve with $\varepsilon = 1/64$, $\gamma = 5 \times 10^{-4}$, $H = 1/16$, $L = 20$. It is important to remark that the results showed in Figure 5 are obtained for $\varepsilon = 1/64$ (hence we obtain $\bar{\sigma}^{\varepsilon,H}$, $\varepsilon = 1/64$). However, in order to well visualize the results and compare the profile of the multiscale tensor with the one shown in Figure 5, we plot $A(\bar{\sigma}^{\varepsilon,H}, x/\varepsilon')$, where $\varepsilon' = 1/8$. We can see a

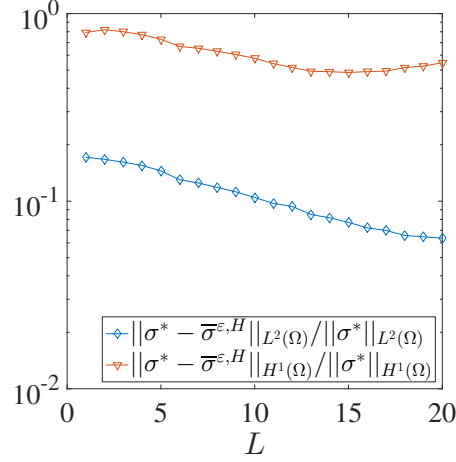


Figure 9: Error behaviour with respect of the number of Dirichlet conditions L .

good agreement between our solution and the true tensor shown in Figure 10.

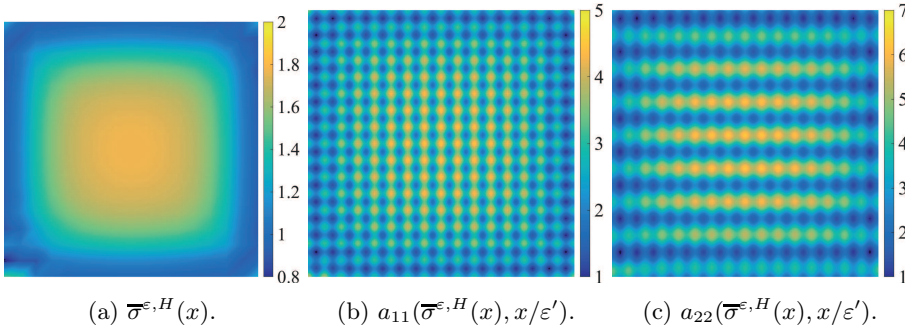


Figure 10: The approximated solution $\bar{\sigma}^{\varepsilon,H}$ and the two components $a_{11}(\bar{\sigma}^{\varepsilon,H}, x/\varepsilon')$ and $a_{22}(\bar{\sigma}^{\varepsilon,H}, x/\varepsilon')$ of the multiscale tensor ($H = 1/16$, $\varepsilon = 1/64$, $\varepsilon' = 1/8$).

5.3. 2D non-affine parametrization. For the second experiment we consider a non-affine parametrization of the multiscale tensor. In this case the function σ^* controls the orientation of the oscillations of the full tensor A^ε , which is defined as follows,

$$\begin{aligned}
 a_{11}(\sigma^*(x), x/\varepsilon) &= 4 \left(\sin \left(\frac{2\pi \mathbf{e}_1^\top Qx}{\varepsilon} \right) + 1.5 \right), \\
 a_{22}(\sigma^*(x), x/\varepsilon) &= 4 \left(\cos \left(\frac{2\pi \mathbf{e}_1^\top Qx}{\varepsilon} \right) + 1.5 \right), \\
 a_{12}(\sigma^*(x), x/\varepsilon) &= a_{21}(\sigma^*(x), x/\varepsilon) = 0,
 \end{aligned}$$

where $Q = Q(\sigma^*(x))$ is a rotation matrix depending on σ^* and is defined as

$$Q = \begin{pmatrix} \cos(2\pi\sigma^*(x)) & \sin(2\pi\sigma^*(x)) \\ -\sin(2\pi\sigma^*(x)) & \cos(2\pi\sigma^*(x)) \end{pmatrix},$$

and

$$\sigma^*(x) = 1.05 + 0.15x_1.$$

Let us remark that for this parametrization the assumption (2.14) in Theorem 2.8 does not hold. However Theorem 3.4 and Theorem 4.5 are still valid. The exact function σ^* , and the components a_{11}^ε , a_{22}^ε are shown in Figure 11, for $\varepsilon = 1/8$. For solving the

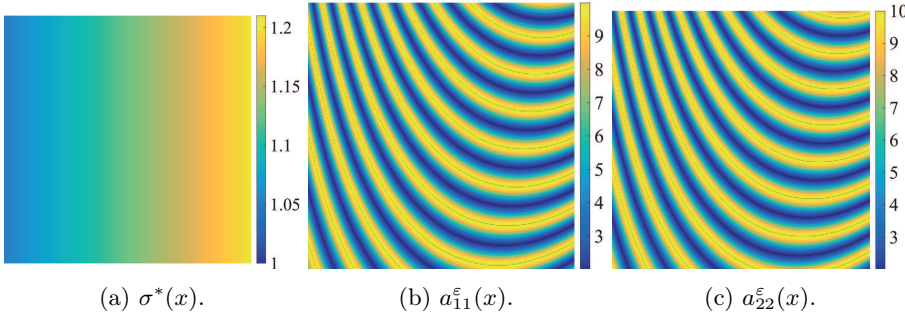


Figure 11: The true field σ^* and the two components a_{11}^ε and a_{22}^ε of the multiscale tensor for the non-affine parametrization ($\varepsilon = 1/8$).

problem we set $\varepsilon = 1/64$, $H = 1/16$, $L = 8$, $\sigma^- = 1$, $\sigma^+ = 1.25$, $\sigma_0 = 1.05$. For this experiment we slightly modify the regularization term. The exact field we want to retrieve changes only with respect to the variable x_1 . Then we assume to know this qualitative property of the unknown and we define the regularization term such that variations with respect to the x_2 direction are more penalized than variations with respect to the x_1 direction. Observe that

$$(5.1) \quad \|\sigma - \sigma_0\|_{H^1(\Omega)}^2 = \|\sigma - \sigma_0\|_{L^2(\Omega)}^2 + \|\partial_{x_1}(\sigma - \sigma_0)\|_{L^2(\Omega)}^2 + \|\partial_{x_2}(\sigma - \sigma_0)\|_{L^2(\Omega)}^2,$$

then instead of multiplying the three addends in the right hand side of (5.1) by the same parameter γ , we use different weights for each of the three addends. The new penalty term is then defined as

$$\gamma_1 \|\sigma - \sigma_0\|_{L^2(\Omega)}^2 + \gamma_2 \|\partial_{x_1}(\sigma - \sigma_0)\|_{L^2(\Omega)}^2 + \gamma_3 \|\partial_{x_2}(\sigma - \sigma_0)\|_{L^2(\Omega)}^2,$$

and for the experiment we are considering we adopt $\gamma_1 = 0.1$, $\gamma_2 = 0.1$, $\gamma_3 = 4$. Let us remark that all the theoretical conclusions are still valid under this regularization term, since it represents an equivalent norm to the $H^1(\Omega)$ -norm. As the parametrization is non-affine, in the offline stage we apply the Empirical Interpolation Method (EIM) to obtain an affine approximation of the tensor, using $tol_{EIM} = 10^{-14}$, where tol_{EIM} is a prescribed tolerance used as stopping criterion for the a posteriori error control in the EIM algorithm. In Figure 12 we show convergence of the residuals in the EIM approximation, and for the reduced basis approximation. In total we get 24 affine

terms for a_{11}^ε , and 25 affine terms for a_{22}^ε , while the reduced space is spanned by $N = 58$ precomputed micro solutions. Therefore for each new value of the unknown, approximating the new homogenized tensor at a macro quadrature point reduces in solving a 58×58 linear system instead of a 4096×4096 linear system, leading to a great saving of computational time. In Figure 13 we show then the approximated solution

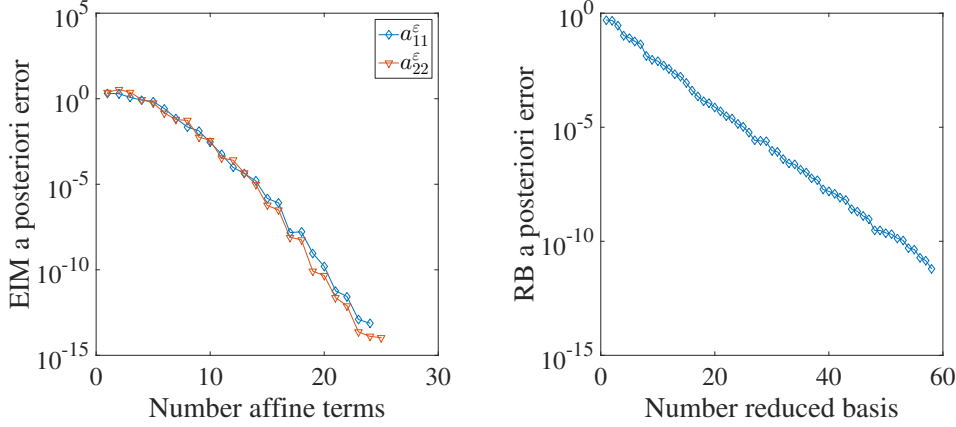


Figure 12: Residuals for the a posteriori error control in the offline stage.

we get by our proposed method. Again we remark that we show the conductivity tensor we retrieve when $\varepsilon = 1/64$ (hence we obtain $\bar{\sigma}^{\varepsilon, H}$, $\varepsilon = 1/64$). However, in order to well visualize the results and compare the profile of the multiscale tensor with the one shown in Figure 11, we plot $A(\bar{\sigma}^{\varepsilon, H}, x/\varepsilon')$, where $\varepsilon' = 1/8$. We can notice that the orientation of the micro oscillations is well captured for most part of the computational domain.

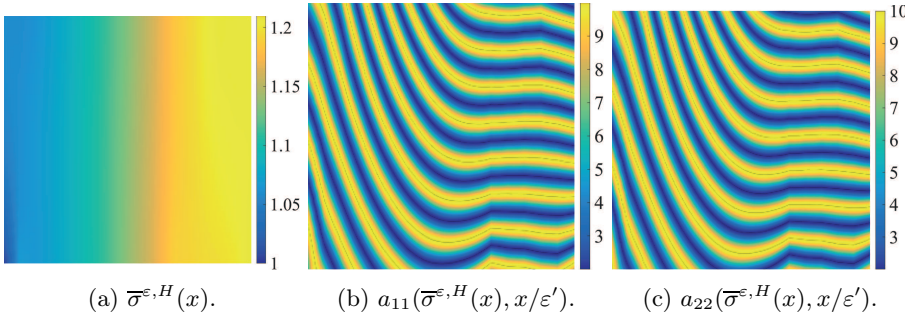


Figure 13: The approximated solution $\bar{\sigma}^{\varepsilon, H}$ and the two components $a_{11}(\bar{\sigma}^{\varepsilon, H}, x/\varepsilon')$ and $a_{22}(\bar{\sigma}^{\varepsilon, H}, x/\varepsilon')$ of the multiscale tensor for the non-affine parametrization ($H = 1/16$, $\varepsilon = 1/64$, $\varepsilon' = 1/8$).

Acknowledgements. The authors are partially supported by the Swiss national foundation.

Appendix. *Proof of Theorem 2.8.* We start by showing (2.6). Let us observe that the homogenized coefficients can be rewritten in the form

$$(5.2) \quad a_{ij}^0(t) = \frac{1}{|Y|} \int_Y A(t, y) (\mathbf{e}_j - \nabla_y \chi_j(t, y)) \cdot (\mathbf{e}_i - \nabla_y \chi_i(t, y)) \, dy.$$

Differentiating (5.2) with respect to the variable t we obtain after a straightforward calculation

$$(5.3) \quad \partial_t a_{ij}^0(t) = \frac{1}{|Y|} \int_Y (\partial_t A(t, y)) (\mathbf{e}_j - \nabla_y \chi_j(t, y)) \cdot (\mathbf{e}_i - \nabla_y \chi_i(t, y)) \, dy.$$

Then from Holder's inequality we get

$$\begin{aligned} & \operatorname{ess\,sup}_{t \in [\sigma^-, \sigma^+]} |\partial_t a_{ij}^0(t)| \\ & \leq \operatorname{ess\,sup}_{t \in [\sigma^-, \sigma^+]} \|\partial_t A(t, \cdot)\|_{L^\infty(Y)} \|\mathbf{e}_j - \nabla_y \chi_j(t, \cdot)\|_{L^2(Y)} \|\mathbf{e}_i - \nabla_y \chi_i(t, \cdot)\|_{L^2(Y)}, \end{aligned}$$

and by using Lax-Milgram theorem, triangle inequality and (2.11) we obtain

$$\begin{aligned} & \operatorname{ess\,sup}_{t \in [\sigma^-, \sigma^+]} |\partial_t a_{ij}^0(t)| \\ & \leq \operatorname{ess\,sup}_{t \in [\sigma^-, \sigma^+]} \|\partial_t A(t, \cdot)\|_{L^\infty(Y)} (1 + \alpha^{-1} \|A(t, \cdot) \cdot \mathbf{e}_j\|_{L^\infty(Y)}) (1 + \alpha^{-1} \|A(t, \cdot) \cdot \mathbf{e}_i\|_{L^\infty(Y)}) \\ & \leq E_1 (1 + \alpha^{-1} E_1)^2 = C_1. \end{aligned}$$

Now, let $t, s \in [\sigma^-, \sigma^+]$. From (5.3) and Hölder's inequality we have

$$\begin{aligned} & |\partial_t a_{ij}^0(t) - \partial_t a_{ij}^0(s)| \\ & \leq \|\partial_t A(t, \cdot) - \partial_t A(s, \cdot)\|_{L^\infty(Y)} \|\mathbf{e}_j - \nabla_y \chi_j(t, \cdot)\|_{L^2(Y)} \|\mathbf{e}_i - \nabla_y \chi_i(t, \cdot)\|_{L^2(Y)} \\ & \quad + \|\partial_t A(s, \cdot)\|_{L^\infty(Y)} \|\nabla_y (\chi_j(t, \cdot) - \chi_j(s, \cdot))\|_{L^2(Y)} \|\mathbf{e}_i - \nabla_y \chi_i(t, \cdot)\|_{L^2(Y)} \\ & \quad + \|\partial_t A(s, \cdot)\|_{L^\infty(Y)} \|\mathbf{e}_j - \nabla_y \chi_j(s, \cdot)\|_{L^2(Y)} \|\nabla_y (\chi_i(t, \cdot) - \chi_i(s, \cdot))\|_{L^2(Y)}. \end{aligned}$$

Now, from the weak definition of the solution of the micro problems, we derive for each $i = 1, \dots, d$, $s, t \in [\sigma^-, \sigma^+]$, $\forall v \in W_{per}^1(Y)$

$$\begin{aligned} \int_Y A(t, y) \nabla_y (\chi_i(t, y) - \chi_i(s, y)) \cdot \nabla_y v \, dy &= \int_Y (A(t, y) - A(s, y)) \mathbf{e}_i \cdot \nabla_y v \, dy \\ & \quad + \int_Y (A(s, y) - A(t, y)) \nabla_y \chi_i(s, y) \cdot \nabla_y v \, dy. \end{aligned}$$

By choosing $v = \chi_i(t, y) - \chi_i(s, y)$, using Hölder's inequality and (2.11) we obtain

$$\begin{aligned} \|\nabla_y (\chi_i(t, \cdot) - \chi_i(s, \cdot))\|_{L^2(Y)} &\leq \alpha^{-1} \|\partial_t A\|_{L^\infty([\sigma^-, \sigma^+]; L^\infty(Y))} (1 + \alpha^{-1} \|A(s, \cdot) \cdot \mathbf{e}_i\|_{L^\infty(Y)}) |t - s| \\ &\leq \alpha^{-1} E_1 (1 + \alpha^{-1} E_1) |t - s| \\ &= C_2 |t - s|. \end{aligned}$$

Using this latter result and the previous inequality gives

$$\begin{aligned} |\partial_t a_{ij}^0(t) - \partial_t a_{ij}^0(s)| &\leq (C_1 + 2E_1(1 + \alpha^{-1} E_1)C_2) |t - s| \\ &= C_1(1 + 2\alpha^{-1} E_1) |t - s| = C_3 |t - s|, \end{aligned}$$

and (2.6) follows.

The condition of uniform ellipticity, namely

$$\alpha|\xi|^2 \leq A^0(t)\xi \cdot \xi, |A^0(t)\xi| \leq \beta|\xi|, \quad \text{for a.e. } t \in [\sigma^-, \sigma^+], \xi \in \mathbb{R}^d,$$

follows from a well known property of the homogenized tensor (see for example Theorem 6.1 in [13]).

Finally we show that the condition of monotonicity with respect to the variable t holds. From (5.3), by using the notation $\varphi_i = (\mathbf{e}_i - \nabla_y \chi_i(t, y))$, $i = 1, \dots, d$, we have that

$$\partial_t a_{ij}^0(t) = \frac{1}{|Y|} \int_Y \partial_t A(t, y) \varphi_j \cdot \varphi_i \, dy.$$

Since $\partial_t A(t, y)$ is symmetric $\partial_t A^0(t)$ is also symmetric. Then, given $\xi \in \mathbb{R}^d$,

$$\begin{aligned} \partial_t A^0(t)\xi \cdot \xi &= \xi^T \partial_t A^0(t)\xi \\ &= \frac{1}{|Y|} \int_Y \sum_{j=1}^d \sum_{i=1}^d \xi_i \varphi_i^T \partial_t A(t, y) \xi_j \varphi_j \, dy \\ &= \frac{1}{|Y|} \int_Y \left(\sum_{i=1}^d \xi_i \varphi_i \right)^T \partial_t A(t, y) \left(\sum_{i=1}^d \xi_i \varphi_i \right) \, dy \\ &\geq E_1^{-1} \int_Y \left| \sum_{i=1}^d \xi_i \varphi_i \right|^2 \, dy \geq 0, \quad \text{for any } \xi \in \mathbb{R}^d. \end{aligned}$$

In particular this inequality implies that

$$(5.4) \quad \partial_t A^0(t)\xi \cdot \xi > 0, \quad \text{for any } \xi \in \mathbb{R}^d, \xi \neq 0,$$

as can be shown using a simple argument by contradiction. Indeed, if this was not true, one would have some $\xi \neq 0$ such that

$$\left| \sum_{i=1}^d \xi_i \varphi_i \right| = \left| \sum_{i=1}^d \xi_i (\mathbf{e}_i - \nabla_y \chi_i) \right| = 0.$$

This means that

$$\sum_{i=1}^d \xi_i (y_i - \chi_i) = \text{constant},$$

and then

$$\sum_{i=1}^d \xi_i y_i = \sum_{i=1}^d \xi_i \chi_i + \text{constant},$$

which is impossible since the right hand side is periodic by definition and $\xi \neq 0$. From (5.4) we easily derive (2.8) and the proof is complete. \square

Before proving Lemma 3.1 let us recall Meyer's theorem on regularity of elliptic problems before proving a technical lemma on the continuity of the Dirichlet to Neumann map with respect to parameter, used in Section 3.

THEOREM 5.1. (*N. G. Meyers, 1963, [20,28]*). *Let $\Omega \in \mathbb{R}^d$ be a bounded open set, with a Lipschitz continuous boundary. Let $A \in \mathcal{M}(\alpha, \beta, \Omega)$. There exists a constant $q_1 > 2$, depending on d, Ω, α and β only, such that if u is the unique weak solution of*

$$\begin{aligned} -\nabla \cdot (A\nabla u) &= f && \text{in } \Omega, \\ u &= g && \text{on } \partial\Omega, \end{aligned}$$

and $f \in W^{-1,q'}(\Omega)$, $g \in W^{1/q,q}(\partial\Omega)$, $1/q' + 1/q = 1$, $q \in [2, q_1)$, then $u \in W^{1,q}(\Omega)$ and there exists a constant C_1 , depending on d, Ω, α, β and q only, such that

$$\|u\|_{W^{1,q}(\Omega)} \leq C_1(\|R_g\|_{W^{1,q}(\Omega)} + \|f\|_{W^{-1,q'}(\Omega)}),$$

where R_g denotes the extension of g onto $W^{1,q}(\Omega)$.

Proof of Lemma 3.1. It follows from the weak formulation of $u^0(\sigma_n)$ and $u^0(\sigma)$ that, for all $v \in H_0^1(\Omega)$, we have

$$\int_{\Omega} (A^0(\sigma)\nabla u^0(\sigma) - A^0(\sigma_n)\nabla u^0(\sigma_n)) \cdot \nabla v \, dx = 0.$$

Then

$$\int_{\Omega} A^0(\sigma_n)(\nabla u^0(\sigma) - \nabla u^0(\sigma_n)) \cdot \nabla v \, dx = \int_{\Omega} (A^0(\sigma_n) - A^0(\sigma))\nabla u^0(\sigma) \cdot \nabla v \, dx.$$

By choosing $v = u^0(\sigma) - u^0(\sigma_n) \in H_0^1(\Omega)$, and using Holder's inequality we obtain,

$$\begin{aligned} \|\nabla u^0(\sigma) - \nabla u^0(\sigma_n)\|_{L^2(\Omega)} &\leq \alpha^{-1}C_1\|A^0(\sigma) - A^0(\sigma_n)\|_{L^p(\Omega)}\|R_g\|_{W^{1,q}(\Omega)} \\ (5.5) \qquad \qquad \qquad &\leq \alpha^{-1}C_1E_1\|\sigma - \sigma_n\|_{L^p(\Omega)}\|R_g\|_{W^{1,q}(\Omega)} \\ &\leq C_2\|\sigma - \sigma_n\|_{L^p(\Omega)}, \end{aligned}$$

where $q \in [2, q_1)$ and C_1 come from Theorem 5.1, and p satisfies $1/p + 1/q = 1/2$. We then set $w = A^0(\sigma)\nabla u^0(\sigma) - A^0(\sigma_n)\nabla u^0(\sigma_n)$ and we obtain

$$\begin{aligned} \int_{\Omega} |w|^2 \, dx &= \int_{\Omega} A^0(\sigma_n)(\nabla u^0(\sigma) - \nabla u^0(\sigma_n)) \cdot w \, dx \\ &\quad + \int_{\Omega} (A^0(\sigma) - A^0(\sigma_n))\nabla u^0(\sigma) \cdot w \, dx \\ &\leq \|A^0(\sigma_n)\|_{L^\infty(\Omega)}\|\nabla u^0(\sigma) - \nabla u^0(\sigma_n)\|_{L^2(\Omega)}\|w\|_{L^2(\Omega)} \\ &\quad + \|A^0(\sigma) - A^0(\sigma_n)\|_{L^p(\Omega)}\|\nabla u^0(\sigma)\|_{L^q(\Omega)}\|w\|_{L^2(\Omega)}, \end{aligned}$$

and hence, by using (5.5) we get

$$\begin{aligned} (5.6) \qquad \|A^0(\sigma)\nabla u^0(\sigma) - A^0(\sigma_n)\nabla u^0(\sigma_n)\|_{L^2(\Omega)} &\leq (E_1 + \alpha)C_2\|\sigma - \sigma_n\|_{L^p(\Omega)} \\ &\leq C_4\|\sigma - \sigma_n\|_{L^p(\Omega)}. \end{aligned}$$

where the exponent $q \in [2, Q_1)$ comes from Theorem 5.1, and p satisfies $1/p + 1/q = 1/2$. Observing that $w \in H(\Omega, \text{div})$ and using the continuity of the map $w \in H(\Omega, \text{div}) \mapsto w \cdot \nu \in H^{-1/2}(\partial\Omega)$, we can finally conclude

$$\|\Lambda_{A^0(\sigma)}g - \Lambda_{A^0(\sigma_n)}g\|_{H^{-1/2}(\partial\Omega)} \leq C_3C_4\|\sigma - \sigma_n\|_{L^p(\Omega)}.$$

The desired assertion follows immediately if $r \geq p$. Otherwise, if $r < p$, we can exploit the $L^\infty(\Omega)$ bound of the set U , i.e., for any $\sigma \in U$ we have

$$\int_{\Omega} |\sigma|^p dx \leq (\sigma^+)^{r-p} \int_{\Omega} |\sigma|^r dx.$$

Assume $u^0 \in H^2(\Omega)$. Then due to the regularity assumptions on $A^0(t)$, the admissible set U , and u^0 , we have that the sequence $\{A^0(\sigma_n)\nabla u^0(\sigma_n)\}_{n>0}$ is uniformly bounded in $(H^1(\Omega))^d$. Then there exists a subsequence $\{A^0(\sigma_{n'})\nabla u^0(\sigma_{n'})\}_{n'>0}$ such that

$$A^0(\sigma_{n'})\nabla u^0(\sigma_{n'}) \rightharpoonup \xi \quad \text{weakly in } (H^1(\Omega))^d,$$

for some $\xi \in (H^1(\Omega))^d$, hence

$$A^0(\sigma_{n'})\nabla u^0(\sigma_{n'}) \rightarrow \xi \quad \text{strongly in } (L^2(\Omega))^d.$$

But from (5.6) all subsequence $\{A^0(\sigma_{n'})\nabla u^0(\sigma_{n'})\}_{n'>0}$ must converge to the same limit, hence

$$A^0(\sigma_n)\nabla u^0(\sigma_n) \rightharpoonup A^0(\sigma)\nabla u^0(\sigma) \quad \text{weakly in } (H^1(\Omega))^d,$$

hence

$$A^0(\sigma_n)\nabla u^0(\sigma_n) \cdot \nu \rightharpoonup A^0(\sigma)\nabla u^0(\sigma) \cdot \nu \quad \text{weakly in } H^{1/2}(\partial\Omega),$$

or

$$\Lambda_{A^0(\sigma_n)}g \rightharpoonup \Lambda_{A^0(\sigma)}g \quad \text{weakly in } H^{1/2}(\partial\Omega).$$

Finally the compact injection $H^{1/2}(\partial\Omega) \subset L^2(\partial\Omega)$ yields

$$A^0(\sigma_n)\nabla u^0(\sigma_n) \cdot \nu \rightarrow A^0(\sigma)\nabla u^0(\sigma) \cdot \nu \quad \text{strongly in } L^2(\partial\Omega),$$

or

$$\Lambda_{A^0(\sigma_n)}g \rightarrow \Lambda_{A^0(\sigma)}g \quad \text{strongly in } L^2(\partial\Omega).$$

□

REFERENCES

- [1] ABDULLE, A. On a priori error analysis of fully discrete heterogeneous multiscale FEM. *Multiscale Model. Simul.* 4, 2 (2005), 447–459.
- [2] ABDULLE, A. Heterogeneous multiscale methods with quadrilateral finite elements. In *Numerical Mathematics and Advanced Applications*, A. B. de Castro, D. Gómez, P. Quintela, and P. Salgado, Eds. Springer Berlin Heidelberg, 2006, pp. 743–751.

- [3] ABDULLE, A. The finite element heterogeneous multiscale method: a computational strategy for multiscale PDEs. In *Multiple scales problems in biomathematics, mechanics, physics and numerics*, vol. 31 of *GAKUTO Internat. Ser. Math. Sci. Appl.* Gakkōtoshō, Tokyo, 2009, pp. 133–181.
- [4] ABDULLE, A., AND BAI, Y. Reduced basis finite element heterogeneous multiscale method for high-order discretizations of elliptic homogenization problems. *J. Comput. Phys.* *231*, 21 (2012), 7014–7036.
- [5] ABDULLE, A., AND NONNENMACHER, A. A short and versatile finite element multiscale code for homogenization problems. *Comput. Methods Appl. Mech. Engrg.* *198*, 37–40 (2009), 2839–2859.
- [6] ABDULLE, A., AND VILMART, G. Analysis of the finite element heterogeneous multiscale method for quasilinear elliptic homogenization problems. *Math. Comp.* *83*, 286 (2014), 513–536.
- [7] ALESSANDRINI, G., AND GABURRO, R. Determining conductivity with special anisotropy by boundary measurements. *SIAM J. MATH. ANAL.* *33*, 1 (2001), 153–171.
- [8] ASTALA, K., AND PÄIVÄRINTA, L. Calderón’s inverse conductivity problem in the plane. *Ann. of Math.* *163* (2006), 265–299.
- [9] BENSOUSSAN, A., LIONS, J.-L., AND PAPANICOLAOU, G. *Asymptotic analysis for periodic structures*. North-Holland Publishing Co., Amsterdam, 1978.
- [10] BYRD, R. H., HRIBAR, M. E., AND NOCEDAL, J. An interior point algorithm for large-scale nonlinear programming. *SIAM J. Optim.* *9*, 4 (1999), 877–900.
- [11] CALDERÓN, A. P. On an inverse boundary value problem. In *Seminar on Numerical Analysis and its Applications to Continuum Physics (Rio de Janeiro, 1980)*. Soc. Bras. Mat., 1980, pp. 65–73.
- [12] CAREY, G. F., CHOW, S.-S., AND SEAGER, M. K. Approximate boundary-flux calculations. *Computer Methods in Applied Mechanics and Engineering* *50*, 2 (1985), 107–120.
- [13] CIORANESCU, D., AND DONATO, P. *An introduction to homogenization*, vol. 17 of *Oxford Lecture Series in Mathematics and its Applications*. Oxford University Press, New York, 1999.
- [14] COLTON, D., ENGL, H., LOUIS, A. K., MCLAUGHIN, J., AND RUNDELL, W. *Surveys on Solution Methods for Inverse Problems*. Springer-Verlag, Wien, 2000.
- [15] DESBRUN, M., DONALDSON, R. D., AND OWHADI, H. Modeling across scales: Discrete geometric structures in homogenization and inverse homogenization. In *Multiscale Analysis and Nonlinear Dynamics: From Genes to the Brain*, M. M. Z. Pesenson, Ed. Wiley-VCH Verlag GmbH & Co. KGaA, Weinheim, Germany, 2013.
- [16] ENGL, H. W., HANKE, M., AND NEUBAUER, A. *Regularization of Inverse Problems*. Kluwer, 1996.
- [17] EVANS, L. C., AND GARIEPY, R. F. *Measure Theory and Fine Properties of Functions*. CRC Press, Boca Raton, 1992.
- [18] FITZPATRICK, B. G. Bayesian analysis in inverse problems. *Inverse Problems* *7* (1991), 675–702.
- [19] FREDERICK, C. A., AND ENGQUIST, B. Numerical methods for multiscale inverse problems. arXiv:1401.2431v2 [math.NA], 2015.
- [20] GALLOUET, T., AND MONIER, A. On the regularity of solutions to elliptic equations. *Rend. Mat. Appl.* *19*, 4 (2000), 471–488.
- [21] GEHERE, M., JIN, B., AND LU, X. An analysis of finite element approximation in electrical impedance tomography. *Inverse Problems* *30*, 4 (2014).
- [22] GREPL, M. A., MADAY, Y., NGUYEN, N. C., AND PATERA, A. T. Efficient reduced-basis treatment of nonaffine and nonlinear partial differential equations. *ESAIM: Mathematical Modelling and Numerical Analysis-Modélisation Mathématique et Analyse Numérique* *41*, 3 (2007), 575–605.
- [23] HANSEN, C. Analysis of discrete ill-posed problems by means of the L-curve. *SIAM Review* *34*, 4 (1992), 561–580.
- [24] HANSEN, C., AND O’LEARY, D. P. The use of the L-curve in the regularization of discrete ill-posed problems. *SIAM J. Sci. Comput.* *14*, 6 (1993), 1487–1503.
- [25] JIKOV, V. V., KOZLOV, S. M., AND OLEINIK, O. A. *Homogenization of differential operators and integral functionals*. Springer-Verlag, Berlin, Heidelberg, 1994.
- [26] KAIPIO, J., AND SOMERSALO, E. *Statistical and Computational Inverse Problems*. Applied Mathematical Sciences, 160. Springer, 2005.
- [27] KOHN, R., AND VOGELIUS, M. Determining conductivity by boundary measurements. 289–298.
- [28] MEYERS, N. G. An L^p -estimate for the gradient of solutions of second order elliptic divergence equations. *Ann. Scuola Norm. Sup. Pisa* *17*, 3 (1963), 189–206.

- [29] NACHMAN, A. Global uniqueness for a two-dimensional inverse boundary value problem. *Ann. of Math.* 143 (1996), 71–96.
- [30] NOLEN, J., PAVLIOTIS, G. A., AND STUART, A. M. Multiscale modelling and inverse problems. *Numerical Analysis of Multiscale Problems*, (2012), 1–34.
- [31] PEHLIVANOV, A. I., LAZAROV, R. D., CAREY, G. F., AND CHOW, S.-S. Superconvergence analysis of approximate boundary-flux calculations. *Numer. Math.* 63 (1992), 483–501.
- [32] SCHERZER, O. The use of Morozov’s discrepancy principle for Tikhonov regularization for solving nonlinear ill-posed problems. *Applied Numerical Mathematics* 4, 5 (1988), 395–417.
- [33] SYLVESTER, J., AND UHLMANN, G. A global uniqueness theorem for an inverse boundary value problem. *Ann. of Math.* 125 (1987), 153–169.

Recent publications:

**MATHEMATICS INSTITUTE OF COMPUTATIONAL SCIENCE AND ENGINEERING
Section of Mathematics**

Ecole Polytechnique Fédérale (EPFL)

CH-1015 Lausanne

- 21.2016** DIANA BONOMI, ANDREA MANZONI, ALFIO QUARTERONI:
A matrix discrete empirical interpolation method for the efficient model reduction of parametrized nonlinear PDEs: application to nonlinear elasticity problems
- 22.2016** JONAS BALLANI, DANIEL KRESSNER, MICHAEL PETERS:
Multilevel tensor approximation of PDEs with random data
- 23.2016** DANIEL KRESSNER, ROBERT LUCE:
Fast computation of the matrix exponential for a Toeplitz matrix
- 24.2016** FRANCESCA BONIZZONI, FABIO NOBILE, ILARIA PERUGIA:
Convergence analysis of Padé approximations for Helmholtz frequency response problems
- 25.2016** MICHELE PISARONI, FABIO NOBILE, PÉNÉLOPE LEYLAND:
A continuation multi level Monte Carlo (C-MLMC) method for uncertainty quantification in compressible aerodynamics
- 26.2016** ASSYR ABDULLE, ONDREJ BUDÁČ:
Multiscale model reduction methods for flow in heterogeneous porous media
- 27.2016** ASSYR ABDULLE, PATRICK HENNING:
Multiscale methods for wave problems in heterogeneous media
- 28.2016** ASSYR ABDULLE, ORANE JECKER:
On heterogeneous coupling of multiscale methods for problems with and without scale separation
- 29.2016** WOLFGANG HACKBUSCH, DANIEL KRESSNER, ANDRÉ USCHMAJEW:
Perturbation of higher-order singular values
- 30.2016** ASSYR ABDULLE, ONDREJ BUDÁČ, ANTOINE IMBODEN:
Multiscale methods and model order reduction for flow problems in three-scale porous media
- 31.2016** DANIEL KRESSNER, ANA ŠUŠNJARA:
Fast computation of spectral projectors of banded matrices
- 32.2016** NICCOLO DAL SANTO, SIMONE DEPARIS, ANDREA MANZONI, ALFIO QUARTERONI:
Multi space reduced basis preconditioners for large-scale parametrized PDEs
- 33.2016** ASSYR ABDULLE, MARTIN HUBER, SIMON LEMAIRE:
An optimization-based numerical method for diffusion problems with sign-changing coefficients
- 34.2016 NEW** ASSYR ABDULLE, ANDREA DI BLASIO:
Numerical homogenization and model order reduction for multiscale inverse problems